Dissertation

on

INVESTIGATION OF EFFECTS OF PROCESS PARAMETERS AND INSERT GEOMETRY ON HARD TURNING OF STEELS

Submitted in partial fulfilment of the requirement for

the award of degree of

MASTER OF ENGINEERING

In

PRODUCTION AND INDUSTRIAL ENGINEERING

Submitted By

MANJOT SINGH CHEEMA

Roll No. 800982012

Under the guidance of

Dr. AJAY BATISH

Professor and Head

Mechanical Engineering Department

Thapar University, Patiala

DEPARTMENT OF MECHANICAL ENGINEERING

THAPAR UNIVERSITY

PATIALA-147004

July 2011

DECLARATION

I hereby declare that the thesis entitled **"INVESTIGATION OF EFFECTS OF PROCESS PARAMETERS AND INSERT GEOMETRY ON HARD TURNING OF STEELS"**, is an authentic record of my study carried out as requirements for the award of the degree of **Master of Engineering (Production and Industrial engineering)** under the guidance of Dr. Ajay Batish, Professor and Head, Department of Mechanical Engineering, Thapar University, Patiala during July 2010 to June 2011. This matter embodied in this report has not been submitted in part or full to any other University or Institute for the award of any degree.

Manjot

Manjot Singh Cheema

This is to certify that above declaration made by the student concerned is correct to the best of my knowledge & belief.

Dr. Ajay Batish
Professor and Head,
Mechanical Engineering Department,
Thapar University, Patiala

Countersigned by

Dr. S. K. Mohapatra
Dean of Academic Affairs
Thapar University, Patiala

ACKNOWLEDGEMENTS

'A Drop of Ink Makes Million Think'

Enumerating and enlisting all the individuals whose contribution went into the completion of the thesis.

A very sincere and honest word of thanks to Dr. Ajay Batish, Professor & HOD, MED for his constructive suggestions and invaluable guidance in making my work a reality. The encouragement and assistance given by him made this a personally rewarding experience. I thank him for his support and constant inspiration. He not only taught the fundamentals essential for doing the thesis but also helped us to develop as an individual.

I would also like to express my heartfelt gratitude to Sh. Anirban Bhattacharya, for his consistent attention and whole hearted support for his dynamic guidance at each and every step of the thesis. I would like to thank him for his great ideas that contributed very much to the thesis work.

I am thankful to Mr. Akshay Kumar and Miss Maninder Kaur for their cooperation and support during the thesis.

The non teaching staff Mr. Sukhbir Puri and Mr. Desh Raj deserves special thanks for their help during the period of this work.

I would like to give special thanks to Micro Turners Pvt. Ltd., Parwanoo and Sartaj Industries, Chandigarh who helped in performing my experimental as well as analysis work.

I express my sincere regards to my parents and my friends for their support during the thesis.

Finally, I am thankful to "ALMIGHTY" for his blessing that helped me in completing my thesis.

Manjot Singh Cheema

ABSTRACT

Turning of materials having hardness above 50 HRC (Rockwell scale) is known as hard part turning. Due to technological developments in the area of computerised numerically control machines, it very easy to machine precise components. The development of new tool materials is being used to turn the hard materials at high speeds. All this has lead to elimination of grinding process which had longer setup times and hard part turning is the upcoming trend which is much fast and precised.

The present study has been done to study the effect of different input parameters on the desired responses on hard turning of different materials. The effect of hardness, material, depth of cut, nose radius, feed and cutting velocity has been evaluated on the machining force, the surface roughness and dimensional deviation. Taguchi's orthogonal array was used to design the experiment. The effect of all the input parameters on the output responses have been analyzed using the analysis of variance (ANOVA). White layer formation, phase analysis and micro strain developed were also studied. Grey relational analysis and Genetic Algorithms were used to determine the optimum combination of input parameters to get the best result.

CONTENTS

LIST OF FIGURES

LIST OF TABLES

ABBREVATIONS

ANOVA- Analysis of variance

S/N- Signal to noise

SEM - Scanning electron microscopy

HAZ - Heat affected zone

MIAS - Metallurgical image analysing system

XRD – X ray diffraction

GRA - Grey relational analysis

DOC – Depth of cut

SAE – Society of Automotive engineers

AISI - American Iron and Steel Institute

DIN - Deutsche Industrie norm

EN – Euro Norm

CNC – Computerised Numerically Control

NOTATIONS

OA - Orthogonal Array

MSD - Mean Square Deviation

SS - Sum of Squares

CI - Confidence Interval

HB - Higher average response is Better

NB - Nominal value is Best

LB - Lower average response is Better

GA- Genetic Algorithm

CHAPTER 1
INTRODUCTION

1.1 MANUFACTURING

Manufacturing means transformation of raw materials into finished goods for the satisfaction of human needs. To transform the raw material different manufacturing processes are applied because of which the shape, size and physical properties of given material are altered.
Different types of manufacturing process for metals are: -

1. **Metal casting**: - Casting is a manufacturing process where a solid is melted and heated to certain temperature, then poured into a cavity or mould, the molten metal solidifies in the mould and the desired shape is formed.
2. **Metal forming and shaping**: - A simple metallic geometry is transformed into a complex one through plastic deformation. Tools or dies impart pressure on the material to transfer the desired geometry through the tool/material interface. It includes rolling, forging, extrusion, drawing, sheet forming, powder metallurgy, molding etc.
3. **Joining**: - Temporary or permanent joining of same or different materials. It includes welding, brazing, soldering, diffusion bonding, adhesive bonding, mechanical joining etc.
4. **Machining**: - It is the metal removing process. It includes turning, boring, drilling, milling, planing, shaping, broaching, grinding etc
5. **Finishing operations**: - It means improving the surface finish of the material. This includes honing, lapping, polishing, burnishing, deburring, coating, plating processes etc.
6. **Material property modification process**: - This process involves changing the property of materials to achieve desirable characteristics. This includes hardening, quenching, annealing, case carburizing etc.
7. **Advanced manufacturing processes**: - It comprises of non traditional machining. It includes ultrasonic machining, abrasive jet machining, chemical, electric discharge machining, electrochemical machining, high-energy beam machining etc. [1-3]

1.2 TURNING

Turning is the process for generating the external surface in which single point cutting tool is moved parallel to the axis of the rotating workpiece. The workpiece is holded in the chuck and tool may be holded in the tool post in case of lathes or in the turret in case of a Computerised Numerically controlled (CNC) turning centre. [2-5]

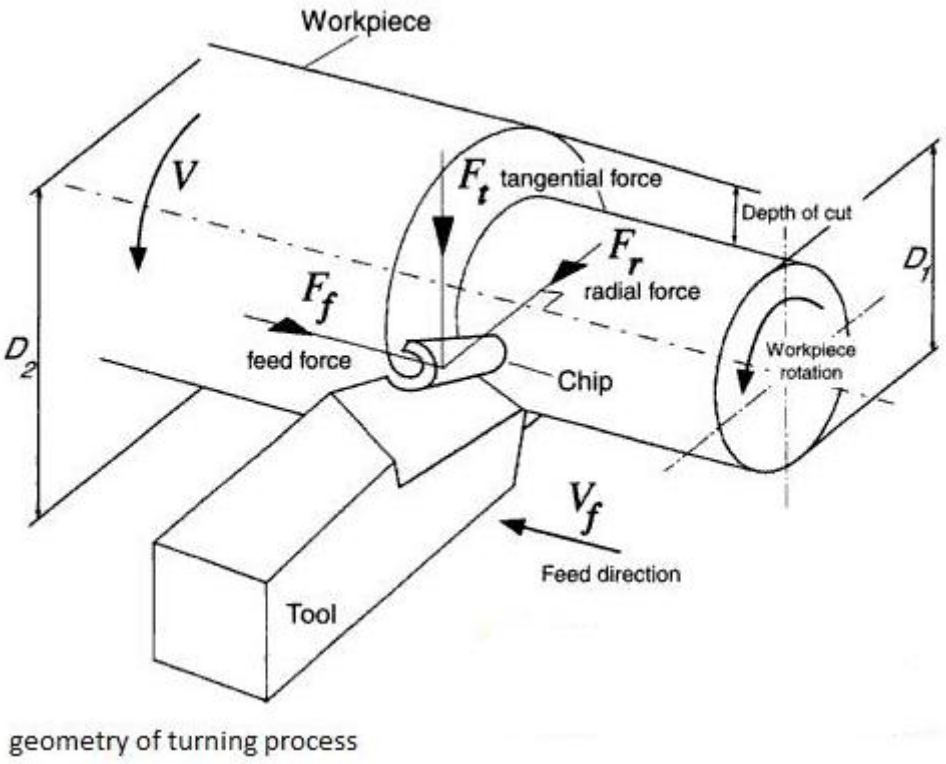

Figure 1.1: Showing the different forces acting on the workpiece during turning. [4]

1.2.1 Cutting forces in Turning

The cutting forces can be resolved into three components

1. The tangential force.
2. The feed force.
3. The radial force.

Tangential force acts in the direction of cutting velocity vector.

Feed force is also known as axial force. It acts in direction of longitudinal feed. Power required in this is less compared to tangential force.

Radial force acts in a radial direction and tends to push the tool away from the workpiece. [2] [4, 6]

1.2.2 Factors influencing cutting forces

Cutting speed: - The distance travelled by the tool per unit time is cutting speed. It is the relative velocity between the cutting tool and the workpiece surface. Cutting speed depends upon material of workpiece, tool being used, and the machine power. Units are given by m/min. Tangential force first increases slightly and then decreases with increase in speed.

Feed: - The amount of tool advancement per revolution of job to the surface being machined is the feed. It is given by mm/rev. Feed depends upon depth of cut (rough or finish) and nature of surface finish required. Force changes linearly with feed at higher speeds and at slower speeds the change is exponential.

Depth of cut: - It is the thickness of the material removed in one cut. It is given by mm. Tangential component of force increases in same relation as the depth of cut if ratio of depth of cut and feed is more than four.

Approach angle: - It is the angle between direction of feed and the side cutting edge. The chip size is dependent on approach angle. Tangential component remains constant in range of 90^{o} to 55^{o} but increases slightly for approach angles less than 55^{o}.

Side Rake angle: - It is the angle between the face of the tool and a line parallel with the base of the tool, measured in a plane perpendicular to the base and the side cutting edge. As the value of side rake angle changes from –ve value to +ve value all components of cutting forces decreases.

Back Rake angle: - It is the angle by which face of the tool is inclined to the back side. The direction of chip flow is controlled by this angle.

Nose Radius: - The radius measured in the back rake or top rake plane of a cutting tool. Radial component of force increases for bigger nose radius resulting in increase in tool chatter. [2, 4 and 6]

1.3 TOOL WEAR

It is the change of shape of tool from its original shape during cutting resulting in gradual loss of tool material (Australian Standard, appendix B P35).

The tool failure is mainly due to following reasons: -

a. Crater wear
b. Flank wear
c. Notch wear
d. Chipping

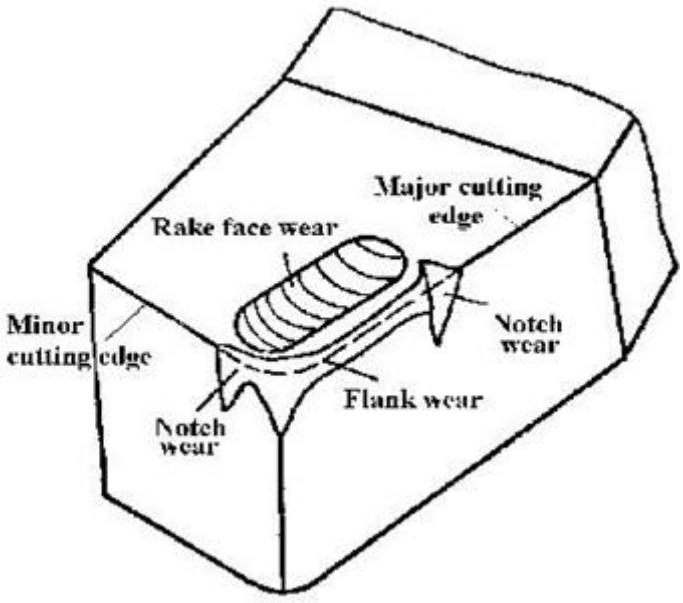

Figure 1.2-
Tool wear phenomena [7]

Crater wear: - The chip flows over the rake face of the insert so this result in friction between the rake face and the chip due to which the rake face starts abrading. This is also known as rake face wear. It gradually affects the insert strength at the end of tool life and it also affects the surface finish.

Flank wear: - This type of wear takes place on the flank and results in a flank land. Wear land formation is not always uniform along the flank land. Flank wear affects the dimensional tolerance of machined parts over a period of time.

Notch wear is combination of both crater wear and flank wear and occurs at the major cutting edge of the insert.

Chipping implies removal of large discrete particles of tool material. Tools subjected to discontinuous cutting are subjected to chipping. [7, 8]

1.4 HARD TURNING

Turning of hard materials above 45 HRC is known as hard turning but usually the metals which are hard turned are in the range of 58-62 HRC. It must be noted that hard doesn't mean difficult but it stands for high hardness materials. The cutting tools used for hard turning are mainly made of Cubic Boron Nitride (CBN), Ceramic and Cermet. The use of tool depends upon the type of requirement like production quantity and type of surface finish required. Ceramic tool inserts can be used when batch production is to be done but CBN tool inserts are used when mass production is to be done. The selection of the tool depends upon the type of application, if intermittent cutting is to be done a low content CBN tool will not work well because of low toughness. So a proper insert should be used as per the required application.

A typical hard turned part which is processed on a correctly configured machine, can have surface finishes below .0003 mm, roundness values of .00025 mm and size control as good as .005 mm. Not all machines are suitable for hard part turning. The machines used should have rigidity, power, efficient chip disposal methods and cooling solutions. Such characteristics cannot be achieved on a normal lathe. So as the technology advances CNC turning centers are being used for hard part turning purposes because they are much convenient and easier to use. [2, 8, 9, 10]

1.4.1 Requirements in hard turning

1. **Use the right equipment**: - Hard turning differs from normal turning. Hard turning may not be possible on normal lathes so for this purpose CNC lathes are to be used.
2. **Maintain high rigidity:** - When the tool comes into contact with the workpiece during hard turning the thrust force increases larger than the feed force. To withstand high forces highly rigid machinery and tooling is required.
3. **Maintain high surface finish: –** Surface roughness is the distance between valley to peak of the feed mark. The peak to valley formation is because of the shape of the cutting edge. When tool wear takes place this phenomenon worsens. Accuracy of the spindle should be there and proper chucking should be done. Surface finish improves at higher speeds.
4. **Avoid tool overhang**: - Tool holder deflection will increase when tool is overhanging so it should be minimized. There should be a rigid method of clamping the tool. [8,10]

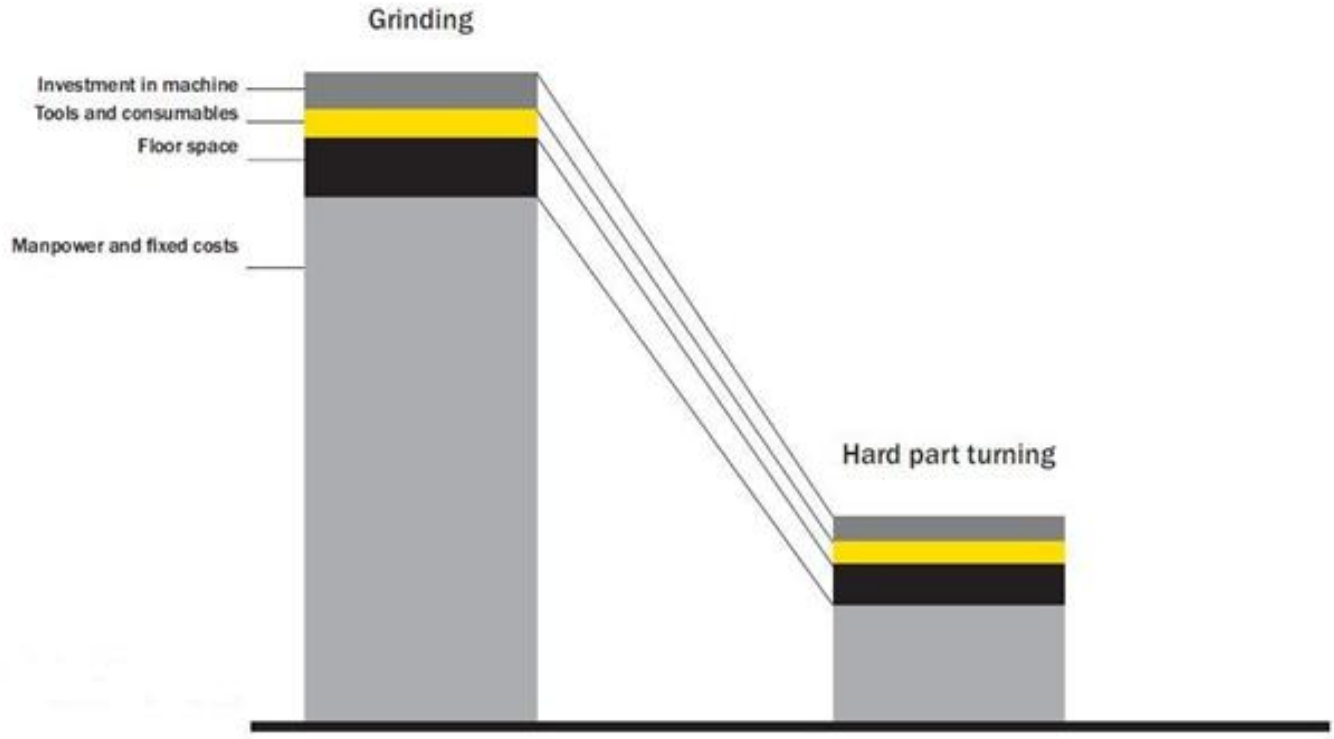

Figure 1.3: - Cost estimates for hard part turning compared to grinding [8]

1.4.2 Advantages of Hard turning

1. When a part is machined and then hardening is done the workpiece tends to distort. Using hard turning the post heat treatment distortion is removed.
2. Hard turning can be used to generate complex contours. Rather than using special designed grinding wheels complex shapes can be generated by single cutting edge.
3. Multiple operations can be done in a single setup so less part handling and less chances of damage.
4. Tooling inventory is low compared to grinding process. [9, 10]

1.4.3 Hard Turning versus Grinding

Hard turning cannot completely replace finish grinding operations but can replace the pre grinding operations. The pre grinding generates worse surface integrity as it causes slight microstructural changes and generates tensile stresses. [9, 10]

Table 1.1: Showing comparative difference between grinding and hard turning process [9]

Grinding	Hard turning
1. Requires longer set up times	1. Short set up times
2. Investment is high	2. Low investment required
3. Cycle time is long	3. Cycle time is short
4. Multiple clamping operations are done	4. Single clamping of the workpiece in chuck is done.
5. Low chip volume	5. High chip volume
6. Dressing of wheel is done so time is wasted	6. No dressing is done. Time is effectively utilised.
7. Not Environmentally friendly because grinding sludge is formed	7. Environmentally friendly , it's a clean process
8. Profile grinding wheel is required	8. Single point cutting tool is required.

1.4.4 Disadvantages of hard turning

1. Hard turning reduces the service life of machined part. Because during turning stresses are generated and microstructural changes take place on the machined surface including the formation of white layers.
2. Hard turning with worn out tool should never be done because it generates a larger amount of tensile stresses and microstructural changes (white layers).
3. Tooling inserts used are very costly. [15]

1.4.5 Tools mainly used for hard turning

1. Coated carbides

Coated carbide consists of three main parts:-

a. Substrate
b. Type of coating
c. Insert geometry

Substrate material is the base material used in carbide insert. Tungsten carbide or cemented carbide is the commonly used substrate material. The substrate material is not very important because the coatings are very efficient in cutting.

The various coating materials applied are Titanium Carbide (TiC), Titanium Carbonitride (TiCN), Titanium Aluminum Nitride (TiAlN), Titanium Nitride (TiN), and Aluminium Oxide (Al_2O_3). The coating of the material is done by Chemical Vapour Deposition (CVD) or Physical Vapour Deposition (PVD).

2. Cubic boron nitride (CBN) tool

The CBN is second hardest material after diamond. It is developed by human under the same pressure and temperature at which diamond is formed. It retains hardness at high temperatures greater than 1000^o. So it is most commonly used tool material for turning hard materials. It can be used for both rough as well finished turning. Conventional materials which can be easily turned should not use CBN tools. CBN tool produces excellent surface finishes and these perform well on big thermal shock.

3. Ceramic cutting tool

These are made from finely powdered aluminium oxide particles with the process of sintering. It is also combined with titanium carbide to form a composite which is known as cermet. These tools can be used for very high speeds as it has high hot hardness. Table 1.2 shows the comparison between CBN insert and ceramic insert. Ceramics can be divided into following categories

a. Aluminium Oxide or white ceramics-

This insert is composed of pure alumina along with it zirconia is added to impart toughness to it. It has a dense and fine structure which has high wear resistance.

Applications- used mainly for turning, boring and grooving of cast iron. It is mainly used for machining of cast iron.

b. Aluminium Carbide and Titanium Carbide mixed grade

This insert comprises of Al_2O_3 and TiC. Increased TiC content and finer structure gives it a long tool life and less tool wear. Titanium nitride coating is also done to lessen the wear. It has good hardness and higher abrasion resistance.

Applications- For turning of heat resistant materials, gray cast iron, hardened materials upto 65 HRc.

c. Titanium Carbide ceramics.

This insert mainly comprises of TiC. It is used on cutting range of 150 m/min to 400 m/min.

Applications – mainly used for ductile cast iron.

d. Aluminium Oxide and Silicon Carbide ceramics.

This is a fine grain ceramic with Titanium Nitride coating mainly used for hard part machining.

Applications- mainly used for continuous cutting and hard part machining. [11-14]

Table 1.2: Comparison between CBN and ceramic tools [16]

Constraint	CBN	Ceramic
Cost	Ten times costly than ceramic	Cheap
Type of operations performed	Roughing, finishing and interrupted cuts	Cannot be used for interrupted cuts
Cutting speed	Requires high cutting speed to work	Can work at less speed
Quantity to be used for	Can be used for bigger lots.	Can be used for small lots where cost is a consideration.
Finishing cuts	Cannot work on low feeds. Can be used to achieve tolerance less than 25 microns.	Work excellent on low feeds and produce a good surface finish.
Material removal rates	High	High

CHAPTER 2
LITERATURE REVIEW

Davim et al. [17] used Response Surface Methodology (RSM) to develop model for predicting the surface roughness, specific cutting force, tool wear, power and machining force. The authors used AISI D2 as work material and used TiN based wiper tool. Selecting cutting speed, feed rate and machining time as parameters and keeping the depth of cut constant, the experiments performed showed that surface roughness value is proportional to feed rate. Flank and crater wear of the tool occurs at high cutting speed. The machining force and the power were more sensitive to feed rate as compared to cutting speed. With increase in machining time the specific cutting force increases as tool wears.

Singh and Rao [18] also developed a surface roughness prediction model by using Response Surface Methodology (RSM). The model developed considered cutting speed, feed and tool geometry (effective rake angle and nose radius) as the parameters. AISI 52100 material and mixed ceramic inserts were used for turning on a high power lathe. The model helped to select the tool geometry so that optimum results can be obtained during hard turning.

In another paper [19] the authors used genetic algorithms to develop a program in c language for optimizing the tool geometry and cutting parameters. The program develop can be used for process planning of products (CAPP).

Chavoshi and Tajdari [20] predicted the surface roughness model by the reverse Artificial Neural Network (ANN) model. Hard turning was done on AISI 4140 using CBN cutting tool. Two parameters – spindle speed and hardness were considered. Experiments conducted showed that the reverse ANN model was more accurate than the regression model. Spindle speed had less effect on surface roughness. Hardness and surface roughness shows a parabolic relationship. First decreased and then increased.

Zhang and Liang [21] developed a model for predicting the 3-dimensional oblique cutting forces and later on validated the results by comparing with the experimental values. The authors also determined the Johnson Cook and wear constants to calibrate the results and predict the tool wear accurately. Mixed Integer Evolutionary Algorithm (MIEA) approach was used in the model. Different low CBN tool inserts with different chamfer angles and

nose radius were used. Other parameters were cutting speed, depth of cut and feed rate. Workpiece material was AISI 1053. The surface roughness values predicted deviated greatly from the experimental results.

Ozel et al. [22] studied the effect of cutting edge geometry, workpiece hardness, feed rate and cutting speed on surface roughness and forces in hard turning of AISI H13 hot work tool steel which was hardened to 50 and 55 HRC .The CBN cutting inserts used had different type of edge geometries like honed, chamfer, chamfer and honed combined and sharp. The results showed that a combination of honed edge geometry and lower workpiece hardness gave better surface finish. Lower cutting speed and lower feed rate results in lower tangential force. Cutting edge geometry, workpiece hardness and cutting speed were the factors which affect the force components. Two factor interactions of edge geometry and workpiece hardness, edge geometry and feed rate and cutting speed and feed rate were also studied.

Jang and Hsiao [23] studied the effect of ceramic tools on hard turning of hardened AISI M2 steel. By varying the cutting speed, feed rate and depth of cut the results concluded that a chemical reaction takes place between the ceramic insert flank face and the turned steel, due to which tool wears mainly due to flank wear and crater wear is very small. In the experiment a thermocouple was kept near to tool tip to measure the temperatures. High cutting speeds and high feed rate causes high flank wear resulting in higher cutting temperatures. Depth of cut had the maximum effect on cutting forces. At the chamfer of the insert cutting took place.

Qian and Hossan [24] used Finite Element Analysis (FEA) to determine the effect on cutting force in turning hardened tool steels (AISI 52100, AISI D2, AISI H13, AISI 4340) using CBN tool inserts. Tool geometry (rake angle and edge radius), feed and cutting speed were the other parameters. The FEA results were compared to experimental results. However other parameters like temperature, shear angle, shear stress, plastic strain rate and chip geometry were not considered. Under the same cutting conditions AISI 4340 requires the maximum cutting force and in AISI D2 the lowest cutting force was observed.

Sieben et al. [25] used design and analysis of computer experiments (DACE) for the empirical modelling of hard turning of AISI 6150 steel. PCBN tool was used for this purpose. The different parameters selected were feed, depth of cut and cutting speed. The DACE technique can be used to model complex non linear factors.

Cappellini et al. [26] used AISI 52100 discs to study the formation of white and dark layers in hard cutting. For this purpose Polycrystalline Cubin Boron Nitride (PCBN) inserts were used. The authors found that as the temperature goes above austenizing temperature, the martensite is readily quenched and white layer is formed. Cutting velocity and feed rate were the parameters. The white layers formed were observed under Scanning Electron Microscope (SEM). It was further observed that as the tool wears the thickness of layers increased. As the velocity increased or the feed rate increased thicker white layers were formed and thinner dark layers were formed.

Aramcharoen and Mativenga [27] also studied the white layer formation and hardening effects on hard turning of H13 tool steel with CrTiAlN and CrTiAlN / MoST coated carbide tools which were developed using Physical Vapour Deposition (PVD) process. Experiment performed was done at two different cutting speeds. Hardening effect was less using these inserts compared to uncoated carbide tool. CrTiAlN and CrTiAlN + MoST coatings were successful in minimizing the white layer formation as it decreased the surface temperature and also reduced the surface hardening effect.

Thamizhmanii and Hasan [28] conducted research on hard AISI 440 C martensitic stainless steel and SCM 440 alloy steel and studied the effect of tool wear and forces by turning process. The tool wear mainly took place due to four reasons – abrasion, diffusion, thermal softening and notching at depth of cut. In which flank wear occurred because of abrasion. The chip formation in hard turning is different from that of a conventional turning process. Saw tooth shaped chips are formed and due to these rough saw tooth shaped chips, crater wear takes place. The carbide present in stainless steel was also responsible for the flank wear. Due to more heat generated in turning of stainless steel the forces required was less than the alloy steel.

Sales et al. [29] made a comparison between the different tool inserts on W320 steel. The various inserts used were coated, cemented carbide, mixed ceramic and PCBN-H tools. At different feeds and cutting velocities the flank wear was measured. Different inserts gave different results at same conditions. It was found that cemented carbide tools performed better at low cutting speed and low feed rate. The performance deteriorated when speed was increased. Due to low toughness Mixed ceramic tools did not perform well at any condition. PCBN-H tool performed well at higher cutting speed at low speed they got weared out. Cost plays an important role on selecting the right tool.

Ko and Kim [30] performed experiments to study the effect of CBN- TiN tool on machineability of hardened AISI 52100 steel in intermittent turning. Three different tools with varying ratio of CBN and TiN were used. The variation of cutting forces with cutting speed, feed rate and depth of cut were studied. The feed rate was varied to study its effect on tool wear and surface roughness. The authors found that feed rate did not affect the tool wear. At the end it was observed that tool with low content of CBN is superior to high content CBN tool as it wears less. Tool wear in intermittent cutting takes place due to combined effect of abrasive wear and adhesion of workpiece and tool. As the speed increases the cutting forces decreases.

Aslan et al. [31] performed the optimization of cutting parameters of AISI 4140 steel with Al_2O_3 + TiCN mixed ceramic tool. Taguchi methods were used for designing of the model. The experimental results and data were analyzed with the help of Analysis of Variance (ANOVA). Parameters used were cutting speed, feed and depth of cut. Multiple regression equations represented the relationships between different factors. It was found that tool wear is mainly affected due to cutting speed. Surface roughness was mainly affected by combined interactions of cutting speed – feed rate and feed rate- depth of cut. When the cutting speed was increased the tool wear decreased. Low level of depth of cut, medium rate of feed and high cutting speed should be selected.

Zhang et al. [32] modelled the residual stress profile in finish hard turning of AISI 1053 and AISI 1070. The authors used low CBN content inserts. The factors which affect the residual stress distribution were insert grade, tool geometry, cutting parameters (cutting speed, feed rate and depth of cut), tool wear progression and depth of cut. The modelling for the residual stress profile was done by Back Propagation Neural Networks (BPNN). X-Ray Diffraction (XRD) technique was used to measure the circumferential and longitudinal stresses. The residual stress decreased with depth. BPNN were used to optimize the tool geometries and cutting conditions.

Lalwani et al. [33] conducted experiments to study the effect of cutting parameters (cutting speed, feed rate and depth of cut) on cutting forces (feed force, thrust force and cutting force) and surface roughness in finish hard turning using coated ceramic inserts on MDN 250 maraging steel. A linear model was developed for the feed force, thrust force and cutting force while for the surface roughness a quadratic model was developed. The depth of cut contributed mainly in the feed force model, feed rate contributed mainly in cutting force,

thrust force model and surface roughness model. Cutting speed had no major effect on cutting forces and surface roughness.

Yallese et al. [34] studied the effect of different cutting parameters (feed, depth of cut and cutting velocity) on hardened AISI 52100 bearing steel. CBN tool was used. A relationship between flank wear and surface roughness was proposed. High speeds above 280 m/min were not recommended for hard turning. As no coolant is used in hard turning the major heat is taken away by the chips. Roughness is mainly affected by feed rate. The surface quality obtained through CBN tool is better than that obtained by grinding process.

Zhou and Hognas [35] performed experiments to achieve precision hard turning of a bore. Pressurised coolant was used and PCBN tool material insert was used. Pressurised coolant had three functions- it broke the cutting chips and reduced the crater wear, break the heat pathway from chips to bore and to avoid thermal expansion it continuously cooled the workpiece during turning. A separate pump system was used to provide pressurized coolant at 30 – 50 MPa.

Zhou and Andersson [36] made a comparison between different types of cooling methods on Novel abrasion Resistance (N-AR) cast iron. For this a tube shaped workpiece was used and CBN tool insert was used. Two different types of cooling methods- pressurised air cooling and conventional cooling with 15 % emulsion was used. Tool life, cutting forces and part surface roughness were the process outputs. The authors concluded that high pressure and high temperatures at the contact area of workpiece and tool are responsible for tool wear. Water based cooling is more effective in minimizing the tool wear as compared to pressurized air cooling. Dry cutting should be avoided.

Singh and Rao [37] used solid lubricants of graphite and Molybdenum Disulphide MoS_2 to compare, with dry turning for AISI 52100 steel. Mixed ceramic tool was used. Cutting velocity, feed and tool geometry (effective rake angle and nose radius) were the parameters considered. The authors found that surface roughness value decreased on using solid lubricants. The lubricating action provided reduces the friction between workpiece and tool. MoS_2 lubricants showed better results than graphite. Solid lubricants also cause less environmental pollution.

Pytlak [38] developed a multicriteria optimization technique for hard turning of hardened 18 HGT [Poland standard of alloy structural steel] steel. CBN inserts of wiper geometry were used. The model considered the following parameters depth of cut, feed and cutting speed. Optimization criteria were production cost, time per unit and resultant cutting force. Weighted objectives method and Modified distance method was used to develop Pareto sets of solutions. To assure low production cost and low values of cutting forces a hierarchical method was used.

Kumar and Ramamoorthy [39] studied the performance of coated tools during hard turning of AISI 4340 alloy steel using minimum cutting fluid application. Two different nitride coated tools (TiCN and ZrN) metal inserts were used. Cutting fluid was commercially available mineral oil. For minimum fluid lubrication system special system was developed which consisted of fuel pump, mixing chamber, and pressure measuring system. It was observed that in minimum quantity lubrication the surface roughness, cutting forces and cutting temperatures were very less compared to dry and wet turning. High quality components can be developed through minimum cutting fluid application.

Chou and Song [40] studied the effect of tool nose radius on turning of hardened AISI 52100 steel. Tool nose radius is an important factor responsible for white layer formation. Ceramic inserts were used for this purpose. Tangential force increases slightly with increase in nose radius. Temperature study was also done around the cutting edge. The white layer formation increased with increase in nose radius and feed. Finer surface finishes were achieved by larger nose radius but tool wear and specific cutting energy increased. New tools lead to deeper white layer formation.

Thamizhmanii et al. [41] studied the effect of hard part turning of SCM 440 induction hardened steel using CBN tool. The authors found that surface roughness is better when combination of high speeds, small depth of cut and low feed is done. The authors also found that at few areas of the workpiece they were unable to determine the surface roughness because of experimental constraints. To account for high surface roughness at that area it was found that the region was of high hardness. Nose wear was much compared to any other wear mechanism.

Yallese et al. [42] conducted experiments using AISI H11 hot work tool steel and they used mixed ceramic tool insert. Response Surface Methodology (RSM) to develop a cutting force model was used. It was observed that in all the experiments radial force was not the principal

force. For greater depth of cut the tangential force becomes the major force. Higher cutting speed, lower feed and lower depth of cut should be used to obtain the best results.

Yallese et al. [43] studied the effect of using mixed ceramic tool and CBN tool to determine the tool wear and effect on surface roughness on hard turning of X200Cr12 material. They developed a relation between the surface roughness and flank wear. Tool wear increased with cutting speed which also resulted in poor surface finish. For longer run using CBN was much beneficial, to produce less quantity ceramic can be used because of economical considerations. CBN worked better at high speeds only.

Summary of all the literature review

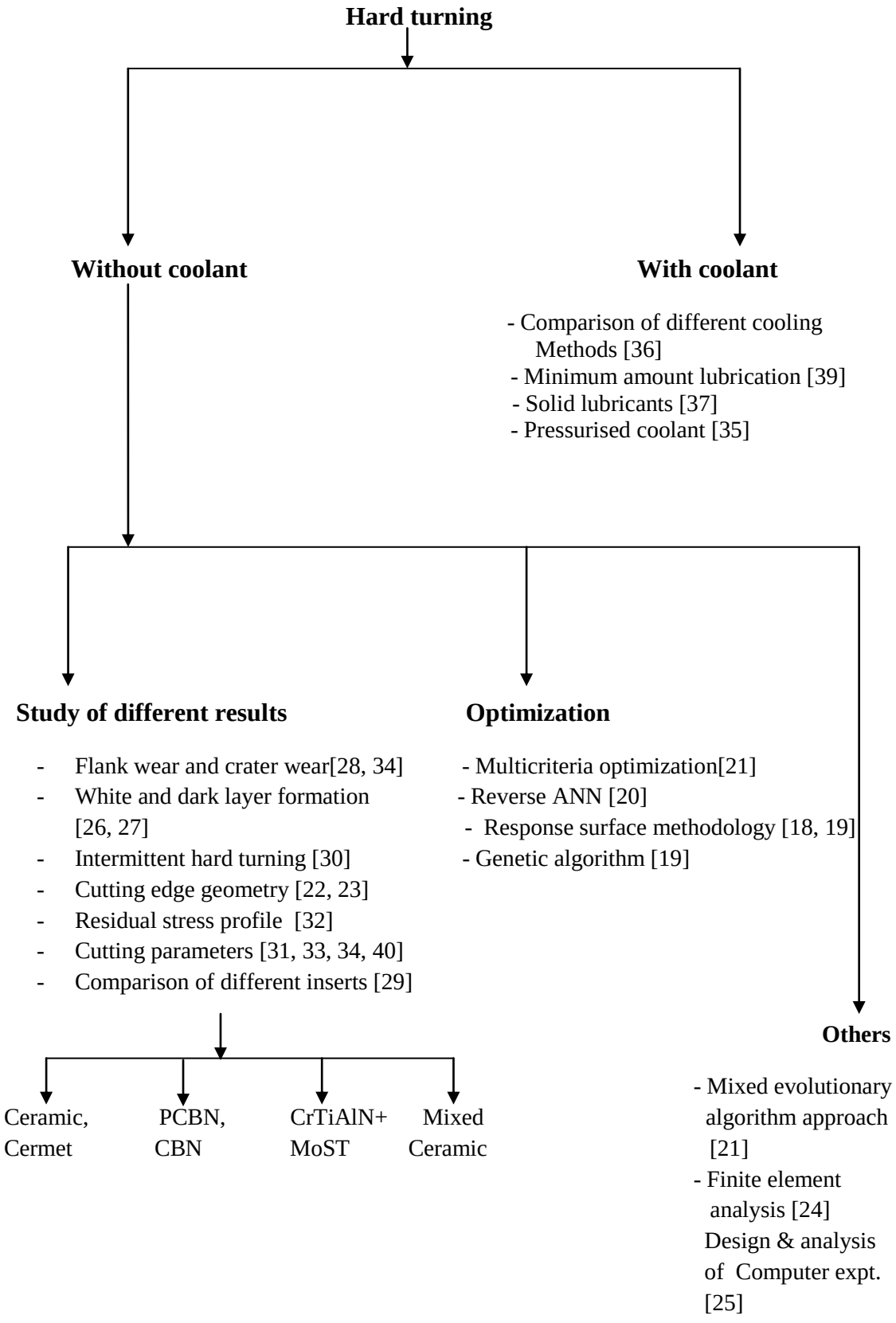

GAPS IN LITERATURE REVIEW

Lots of work has been done on area of hard part turning using various experiments. But very less work has been done in understanding the metallurgical aspects of hard part turning. Further lot of work has been done on the optimization techniques by selecting various input parameters. Many researchers have designed the experiment which includes a study of the various process parameters but no one has designed an experiment which considers the combined effect of hardness, tool nose radius, feed, cutting velocity, depth of cut and material type. Little literature review is available on optimization using genetic algorithms.

PROBLEM FORMULATION

In this thesis work it is proposed to study the hard part turning of three most commonly used materials in Indian Auto industry. The proposed study included the complete analysis of different process parameters like nose radius, depth of cut, feed, cutting speed depth of cut on finish hard turning of EN 9 , EN 31 and SAE 8620 . The metallurgical changes before and after hard turning were studied using XRD, SEM and Leica microscopy techniques. Optimum conditions were identified using Grey Relational Analysis and Genetic algorithm approach.

CHAPTER 3

DESIGN OF STUDY

3.1 PHASES IN THE STUDY

The study can be divided into three phases

1. PHASE 1 : Preliminary study

   This phase aimed at detailed study of hard part machining. The effect of various process parameters on the performance of the process was studied and there working limits were identified.

2. PHASE 2 : Experimental setup

   In this phase the setup to mount the dynamometer on NC machine was developed with attached computer setup. To ensure desired hardness correct method of hardening was done on the material.

3. PHASE 3: Results and analysis

   In this phase the forces and surface roughness were evaluated using ANOVA and the significant and insignificant parameters were determined. The dimensional deviation was studied. Metallurgical analysis was completed to find the phases present in the material after hard turning. White layer formation and surface pattern was also studied. Grey relational analysis and Genetic algorithm were used to get optimum solutions.

3.2 EXPERIMENTAL OUTLINE

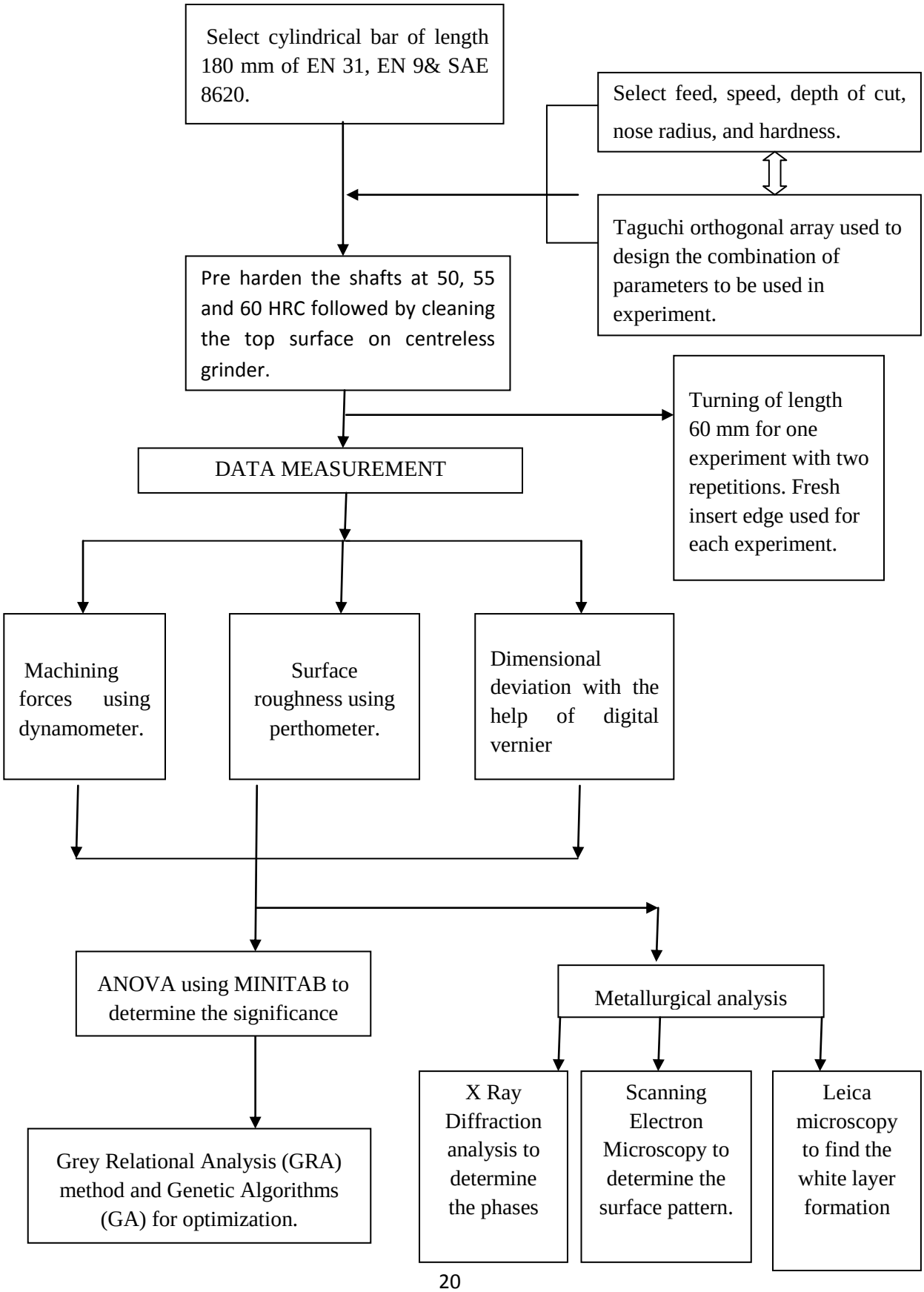

CHAPTER 4

EXPERIMENTAL DESIGN

4.1 METHODOLOGY

The experiment was conducted through design of experiments technique. Taguchi's orthogonal array design was used because it had advantages over full factorial design. The number of experiments conducted was reduced with Taguchi's design as it simplified the fractional factorial design. The effect of various design parameters were studied through this design.

4.2 PROCEDURES OF TAGUCHI METHOD

The brief procedure of Taguchi method is as under

- Identify the objective function.
- Select the factors to be evaluated
- Identification of uncontrollable factors and test conditions
- Selection of levels of controllable and uncontrollable factors.
- Calculate the total degrees of freedom.
- Select the appropriate orthogonal array.
- Assignment of factors to columns.
- Execution of experiments according to the trial conditions in array
- Analyze the result
- Confirmation results [44]

4.3 THE OBJECTIVE FUNCTION

The objective is to determine the effect of hardness, feed, cutting speed, nose radius, depth of cut and workpiece material on the machining forces, surface roughness and dimensional deviation were selected as the output.

4.4 DESIGN OF EXPERIMENTS AND SELECTION OF ORTHOGONAL ARRAY SYSTEM

4.4.1 Degrees of Freedom

The number of freedom in a problem or distribution is the number of parameters which can be independently varied. Degree of freedom determines the number of treatment conditions.
In a single sample if there are n observations and there is one parameter (the mean) which needs to be estimated. n-1 degrees of freedom are left to estimate the variability.

If there are two samples with observations n_1 and n_2. There are two means to be estimated so we will have n_1+n_2 -2 degrees of freedom. [45]

4.4.2 Factors of interest and their levels

The factors which affect the response parameters (forces and surface roughness) with there levels were identified using cause and effect relationship. The aim of experiment was such that all the factors used in past work can be utilised in this experiment. The various parameters were decided according to machine settings and the availability of materials. There were no interactions between the factors to be studied.

Table 4.1: Factors and there levels.

Factors	Levels		
	Level 1	**Level 2**	**Level 3**
Hardness (HRC)	50	55	60
Material	EN 31	SAE 8620	EN 9
Nose radius(mm)-Depth of cut(mm)	0.4-0.075	0.4-0.15	0.8-0.15
Speed(m/min)	75	110	150
Feed (mm/rev)	0.03	0.06	0.1

The third factor combination of nose radius and depth of cut was decided with help of Taguchi's design. The factors which do not have a direct relationship between them can be combined so a combination of nose radius and depth of cut was made.

Every factor had three levels. The minimum required degrees of freedom in the experiment are the sum of all the degrees of freedom of factors. For each factors there are three levels.

The degree of freedom for each factor is 2. For the experiment the number of degrees of freedom calculated was 10 as shown in table 4.2. The orthogonal error to be chosen should have degrees of freedom greater than 10. For the 5 factors with three levels the available orthogonal array that can be used for the experiment was L_{27} which had 26 degrees of freedom.

Table 4.2: Degrees of freedom for various levels

Factors	Units	Degrees of freedom
Hardness	HRC	2
Material		2
Nose radius- Depth of cut	Mm	2
Speed	(m/min)	2
Feed	(mm/rev)	2
Total		10

4.5 ORTHOGONAL ARRAY

The experiment has 5 factors which have 3 levels. If full factorial design was chosen than 5^3=125 experiments would have to be done. If Taguchi's design with an L_{27} orthogonal array was selected only 27 experiments were done. Orthogonal designs allow estimating the effect of each factor on the response independently of all other factors.

Taguchi encourages users to select variables that do not interact with one another, so two factors nose radius and depth of cut were combined to form one factor. If individually they were considered our experimental design would have been changed and there would have been 6 factors which would increase the number of experiments. It was assumed that the factors 'nose radius' and 'depth of cut' have no relationship between them for the levels chosen.

The orthogonal error was chosen using MINITAB 15 software. All the parameters and levels were input and it generated the orthogonal array automatically. The orthogonal array developed is shown in table 4.3.

Table 4.3: L_{27} Experimental design

S.No.	Hardness (HRC)	Material	Nose Radius(mm)-depth of cut(mm)	Cutting speed (m/min)	Feed (mm/rev)
1	50	EN 31	0.4-0.075	75	0.03
2	50	EN 31	0.4-0.075	75	0.06
3	50	EN 31	0.4-0.075	75	0.1
4	50	SAE 8620	0.4-0.15	110	0.03
5	50	SAE 8620	0.4-0.15	110	0.06
6	50	SAE 8620	0.4-0.15	110	0.1
7	50	EN 9	0.8-0.15	150	0.03
8	50	EN 9	0.8-0.15	150	0.06
9	50	EN 9	0.8-0.15	150	0.1
10	55	EN 31	0.4-0.15	150	0.03
11	55	EN 31	0.4-0.15	150	0.06
12	55	EN 31	0.4-0.15	150	0.1
13	55	SAE 8620	0.8-0.15	75	0.03
14	55	SAE 8620	0.8-0.15	75	0.06
15	55	SAE 8620	0.8-0.15	75	0.1
16	55	EN 9	0.4-0.075	110	0.03
17	55	EN 9	0.4-0.075	110	0.06
18	55	EN 9	0.4-0.075	110	0.1
19	60	EN 31	0.8-0.15	110	0.03
20	60	EN 31	0.8-0.15	110	0.06
21	60	EN 31	0.8-0.15	110	0.1
22	60	SAE 8620	0.4-0.075	150	0.03
23	60	SAE 8620	0.4-0.075	150	0.06
24	60	SAE 8620	0.4-0.075	150	0.1
25	60	EN 9	0.4-0.15	75	0.03
26	60	EN 9	0.4-0.15	75	0.06
27	60	EN 9	0.4-0.15	75	0.1

4.6 MATERIALS USED AND HARDENING TECHNIQUE

The materials selected were on the basis that was most commonly used in the Indian auto industry which was hardened. So for experiment purposes following materials were used:-

1. SAE 8620
2. EN 9
3. EN 31

4.6.1 SAE 8620

This is a case hardening alloy steel and it has the following equivalents

EN no.	SAE	AISI	DIN
351	8620	8620	--

Composition in %

C	Mn	P	S	Si	Cr	Ni	Mo
0.18-0.23	0.70-0.90	0.035	0.04	0.15-0.30	0.40-0.60	0.40-0.70	0.15-0.25

Applications

It is a low alloy case hardening steel which can be carburized and hardened to produce a hard wear resistant case with good resistance to shock. Typical uses are: gears, gudgeon pins, shafts, levers, camshafts, drive wheels, clutch plates, etc. [46]

Case Carburizing method of SAE 8620.

Carburizing method is used for low carbon steels at a temperature of 850°C to 900°C by the addition of carbon using salt bath carburizing technique. In this technique hardening was accomplished when high carbon surface layer is quenched to form high carbon- martensitic case which has good wear resistance but it has a soft core.

In this method of carburizing to achieve a case depth of 1 mm the material was kept in the furnace at 800 °C and the salt used was sodium cyanide. After 5 hours it was air cooled and then again reheated at a temperature of 820 °C to hard it.

After Carburizing, Quenching was done using oil. The following Tempering temperatures were used to achieve desired hardness.

60HRC - 130°C

55HRC - 250°C

50 HRC - 400°C

4.6.2 EN 9

The EN 9 steel is a Plain carbon steel and it has the following equivalent

EN no.	SAE	AISI	GOST
9	1055	C 1055	1050-60 Grade 50

Composition in %

C	Mn	P	S
0.50-0.60	0.60-0.90	0.04	0.05

Applications

Used for sprockets and springs, cylinders, cams, crankshafts, small gears, keys etc. This is surface hardened by flame or induction heating. [47]

Induction hardening method of EN 9

Induction hardening method of hardening consists of a copper coil through which high amount of alternating electric current is passed. The workpiece is held between the several turns of copper coil between which it has a rotating motion. The coil also goes up and down and its peed can be controlled so that the desired case depth can be achieved. When alternating current is passed through the coil a magnetic field is generated whose intensity varies periodically with direction and motion. Below the coil there is a nozzle fixed which supplies water so that the steel can be quenched at the same time. The alternating current produces heating effect on the surface and temperature produced is of the order of 800°C to 900°C. The case depth achieved was about 1 mm and the hardness achieved was about 60 to 62 HRC.

Tempering

The hardness achieved is about 60 to 62 HRC when hardening was done. To achieve hardness of 55 HRC and 50 HRC, the shaft was tempered in the tempering furnace or it can be tempered on the machine itself. To temper it in the furnace a temperature of 220° C is maintained in the furnace and then the workpiece is hold for 2 hours. After that the desired hardness is achieved.

For my experiment work the tempering was done itself on the induction hardening machine. The current was passed through coil and than self quenching (quenching in air) was done. After workpiece was removed from the setup and hold in still air for 5 – 10

minutes and hardness achieved was of about 55 HRC. To achieve a hardness of 50 HRC the holding time was about 40 minutes.

4.6.3 EN 31

This is a low and medium alloy steel which has following equivalents:-

EN no.	SAE	AISI	GOST
31	52100	E 52100	Grade 111x15

Composition in %

C	Mn	P	S	Si	Cr
0.98-1.10	0.25-0.45	0.025	0.025	0.15-0.30	1.30-1.60

Applications

Can be oil quenched for sections up to 25 mm diameter and water hardened in larger sections to produce a hard wear resistance surface. Used for: ball and roller bearings, bearing rings, bushes, collets, cams, lathe centres etc. [48]

Hardening method for EN 31

For EN 31 hardening is done at a temperature of 820-860°C directly by heating in the furnace. Quenching is done using an oil medium. Quenching is done at rate faster than the critical rate. Austenite to Martensite transformation takes place.

Then tempering is done at 150°C.

4.7 EXPERIMENTAL SETUP

4.7.1 Workpiece dimensions

The workpiece chosen was of different material. The shafts were pre turned so that two shafts of same material have the same dimensions. The diameter of the shaft was about 26 mm and a length of 18 cm. The size was measured with help of digital vernier micrometer which gave values up to three decimal places. It was found that after hardening scale formation and salt accumulation was done on the shafts. To remove the scale, shafts were grinded on cylindrical grinder. The diameter was maintained during grinding operation and two shafts of same material had the same diameter. Turning length was about 60 mm for one set of experiment. If there was a variation in the diameter it was adjusted by providing offset in the CNC machine program.

4.7.2 Machine R.P.M calculation

After deciding the cutting speed the r.p.m were calculated accordingly. The formula used for calculating the machine r.p.m was

$$v = \frac{\pi d N}{1000} \qquad \text{---------- (Eq. 4.1)}$$

v- cutting velocity in m/min

d- diameter of the shaft in mm

N- rotations per minute

For a shaft having 26 mm diameter the R.P.M values are as calculated in the table 4.4

Table 4.4: r.p.m calculated

Cutting velocity(m/min)	R.P.M calculated
75	918
110	1348
150	1837

4.7.3 Machine Used

4.7.3.1 Machine description

Type: - CNC turning center model 'Jobber xl' developed by ACE designers ltd., Bangalore

Year of make – 2008

The ACE jobber XL CNC machines are very high precision machines used for mass productions. They have the advantage of high production rates, constant surface speeds etc. the important features of this machine include:-

- The bed is made of 25 different cast iron castings which is rigid and provides stability. Bed also ensures easy chip flow and removal. The bed undergoes natural seasoning and stress relieving before assembly.
- The X and Z axis have precision ball screw at both ends. The ball screw is pre tensioned so that the effect of temperature variations can be minimized linear motion guide ways are used to slide the X and Z axis slides. Automatic metered lubrication of balls and guide ways is provided. The axis system is also provided with overloading safety device which protects the machine against application of excessive motion torque on the elements and prevents accidents.
- The electrical system is highly reliable as it uses the best internationally accepted elements. Fanuc AC spindle motor and controller, Fanuc axes motors are used.
- The spindle uses high precision bearings in the front and the rear. The bearings are grease lubricated through life.
- The tailstock is supported on V and flat guide ways and houses a live center. [49]

4.7.3.2 Technical Data

Capacity

Distance between centers (mm): - 400

Maximum turning diameter (mm): - 290

Maximum turning length (mm):- 400

Spindle drive

Spindle motor rated power (kW): – 7.5

Spindle speed (max.): – 3500 r.p.m

Axes Slides

X axis stroke (mm): - 150

Z axis stroke (mm): - 400

Feed rate (inf. Variable) (mm/min):– 0-10000

Rapid traverse rate: X axis (m/min): - 20

Rapid traverse rate: Z axis (m/min): - 20

Turret

No. of stations: - 8

Maximum boring bar dia. (mm): - 40

Tool crossection (mm): - 25 X 25

CNC operating system: - Fanuc 0i Mate- TC

Boring bar holder: - 4 nos.

Facing tool holder: – 2 nos.

OD turning tool: -8 nos.

Standard features

Hydraulic power chuck ϕ 200 mm

AC spindle & axes drives

High speed bi-directional tool for turrets. [49]

Figure 4.1: ACE CNC jobber xl on which experiment was performed

Figure 4.2: shows the Fanuc controller and panel from where the programming is done and all parameters are controlled

4.7.4 Ceramic tool insert Description

1. TaeguTec Ceramic Insert CNGA 431

   CNGA 120404 AB20 - CNGA 432 AB20

   Nose radius- 0.04 mm

   Insert material: CERAMIC - Al_2O_3+ TiCN

   Operation: turning/boring/milling

2. TaeguTec Ceramic Insert CNGA 431

   CNGA 120408 AB20 - CNGA 432 AB20

   Nose radius – 0.08 mm

   Insert material: CERAMIC – Al_2O_3+ TiCN

   Operation: turning/boring/milling

Cutting speed recommended – 100 to 200 m/min

Feed recommended – 0.03 to 2.5 mm/rev.

No Coolant required.

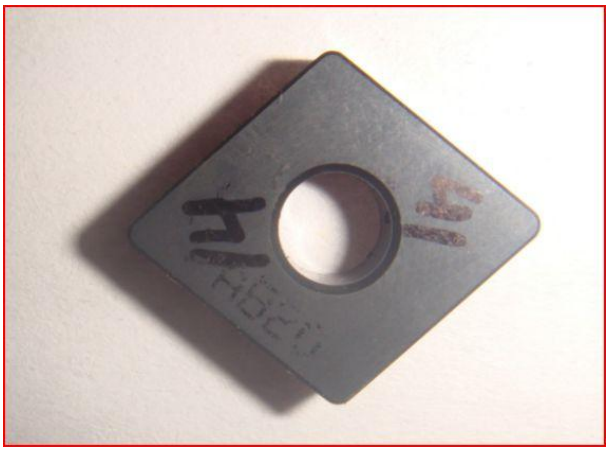

Figure 4.3: CNGA 0.8mm nose radius insert

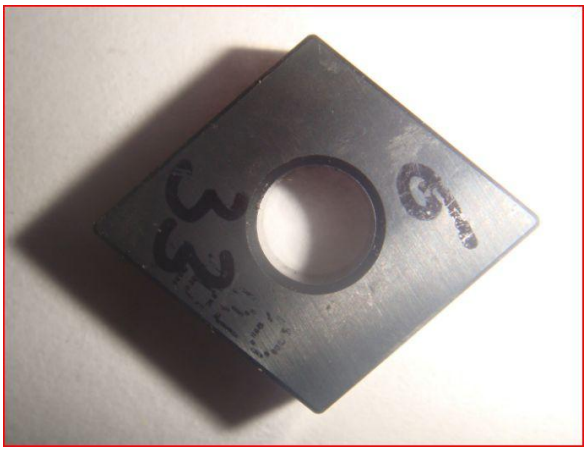

Figure 4.4: CNGA 0.4 mm nose radius.

4.7.4.1 Cutting tool designation

The codes given for tool have a special meaning as shown in table 4.5

C	N	G	A	12	04	08	AB 20
1	2	3	4	5	6	7	8

Table 4.5: Designation of the insert [50]

S. no	Symbol	Meaning	Figure	Description
1	**C**	Insert shape	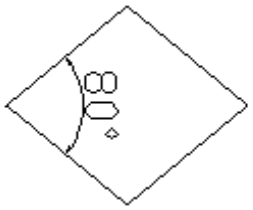	And angle of 80° between the two edges.
2	**N**	Insert Clearance angle	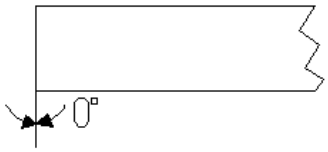	0° angle between the upper and lower edge.
3	**G**	Tolerances	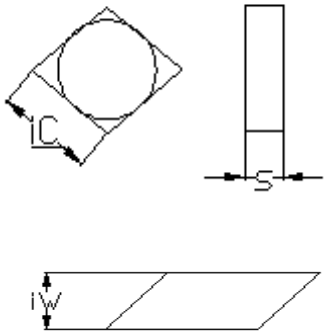	Inscribed circle radius-iC S= ±0.13 iC/iW=±0.025
4	**A**	Insert type		Insert with hole
5	**12**	Insert size-Cutting edge length.	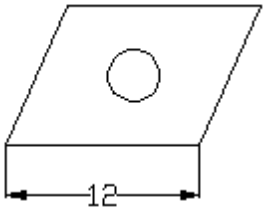	12 mm
6	**04**	Insert thickness	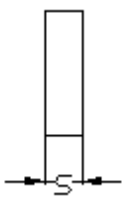	S= 4.76mm
7	**08**	Insert nose radius		0.8 mm
8	**AB 20**	Company grade		

4.7.5 Cutting tool holder description

For turning operations a Sandvik Coromant CoroTurn® RC tool was used. This tool is used for turning and facing applications where cutting loads are heavy. The tool has the following code and it is used only for CNMG inserts

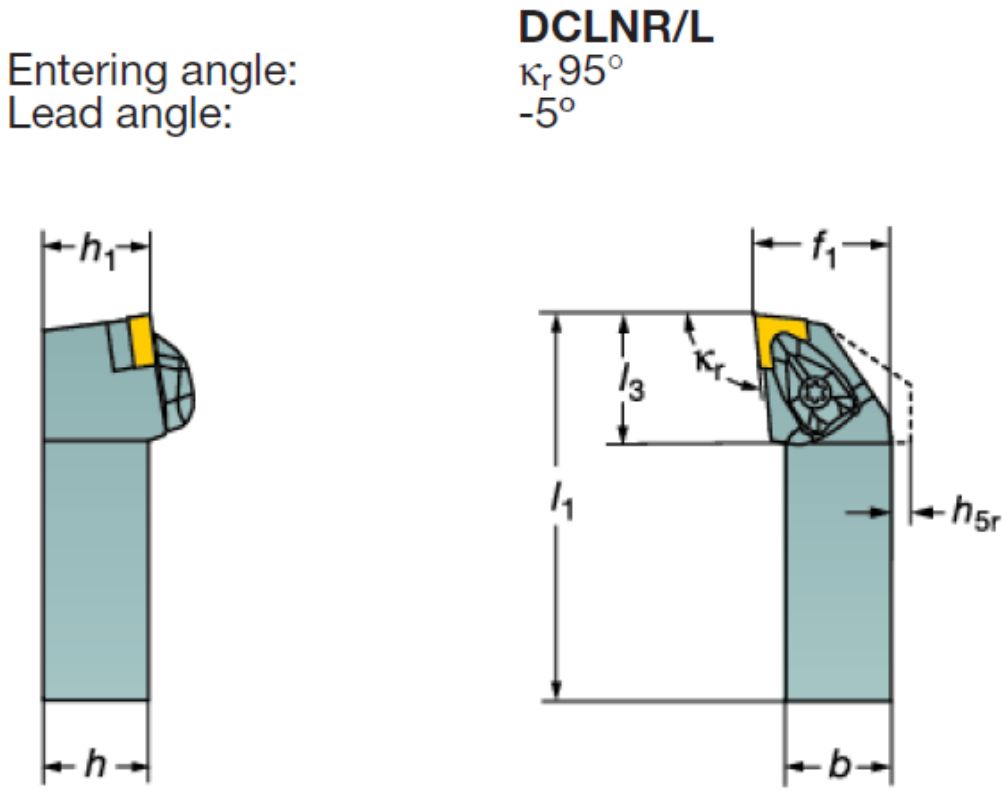

Figure 4.5: shows the tool geometry [51]

The dimensions for the tool are

Ordering code	B	f_1	h	h_1	l_1	l_3
DCLNR/L 2525M 12	25	32	25	25	150	32

4.7.5.1 Tool holder designation [51]

D	C	L	N	R	25	25	M	12
1	2	3	4	5	6	7	8	9

Table 4.6: Tool holder designation

S.No.	SYMBOL	MEANING	FIGURE	DESCRIPTION
1	**D**	Clamping system	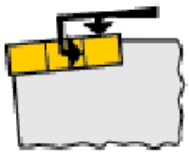 [51]	Top and hole clamping
2	**C**	Insert shape	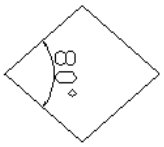	CNMG
3	**L**	Holder style entering angle (lead angle)	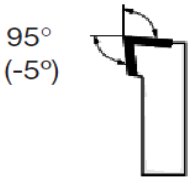 [51]	95°
4	**N**	Insert clearance angle	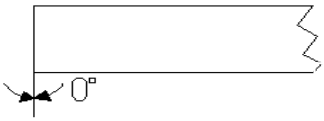	0°
5	**R**	Hand of tool	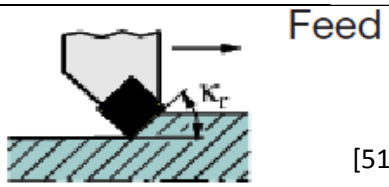 [51]	Right hand tool
6	**25**	Shank size-height	 [51]	25 mm
7	**25**	Shank size-width	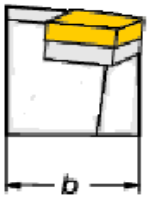 [51]	25 mm
8	**M**	Shank tool length	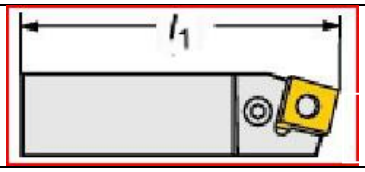 [51]	150 mm
9	**12**	Cutting edge length	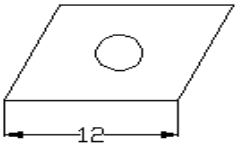	12 mm

4.7.6 Measurement of forces by dynamometer and setup of dynamometer on CNC Turret

Kistler four component Dynamometer type 9272

The three orthogonal components of force and the torque are measured by dynamometer. The four component dynamometer type 9272 used in this is developed by Kistler instruments. The dynamometer has a high natural frequency. Due to its high resolution the smallest dynamic changes in forces and torques can be measured. For measuring the forces the dynamometer setup also contains connecting cable (8 leads) and charge amplifier. The technical data is shown in the table 4.7. [52]

Applications of Kistler 9272

It is used to measure deflection force and moment, cutting force measurements in boring, milling, grinding etc.

figure adapted from Kistler Instrumente manual 2005

Figure 4.6: showing Kistler dynamometer type 9272 which is to be used for measuring forces during hard turning [52]

Table 4.7: showing technical details of Kistler dynamometer type 9272 [52]

Range	Fx, Fy	Kn	–2 … 2
	Fz	kN	0 … 4
Crosstalk	Fx ↔ Fy	%	≤±5
	Fz → Fx,y	%	≤±2
	Fx,y → Fz	%	≤±5
Natural frequency (mounted on flanges)	fn (x,y)	kHz	≈1,5
	fn (z)	kHz	≈4

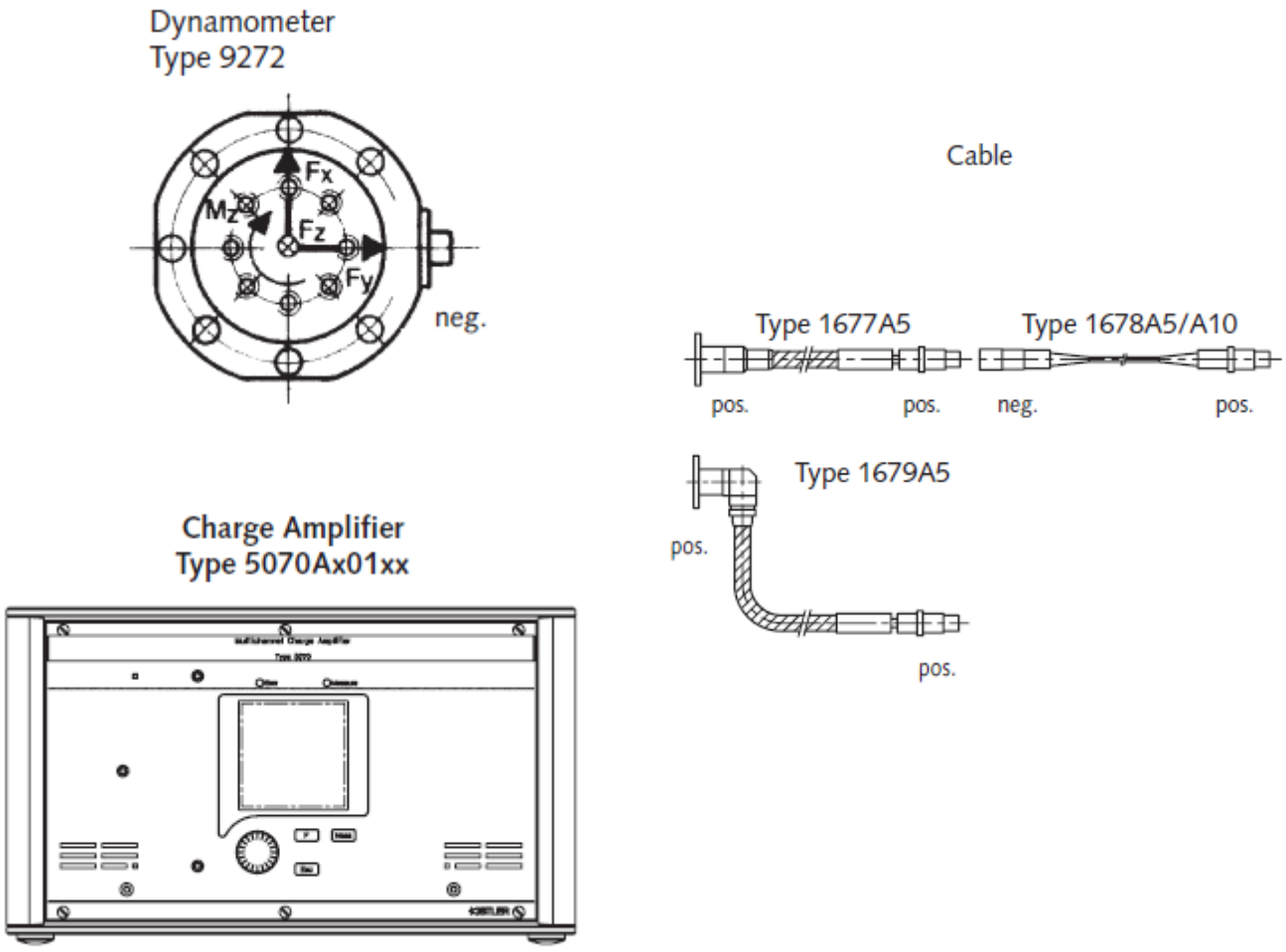

Figure 4.7: Showing the measuring system with dynamometer type 9272 [52]

The dynamometer was clamped on the turret with a special tool shank. The shank was first tightened on the turret station and then dynamometer was attached using two bolts to the shank. After this the special fixture was tightened on the dynamometer face. After that the tool was inserted in the slot of the fixture and then it was also tightened with allen bolts.

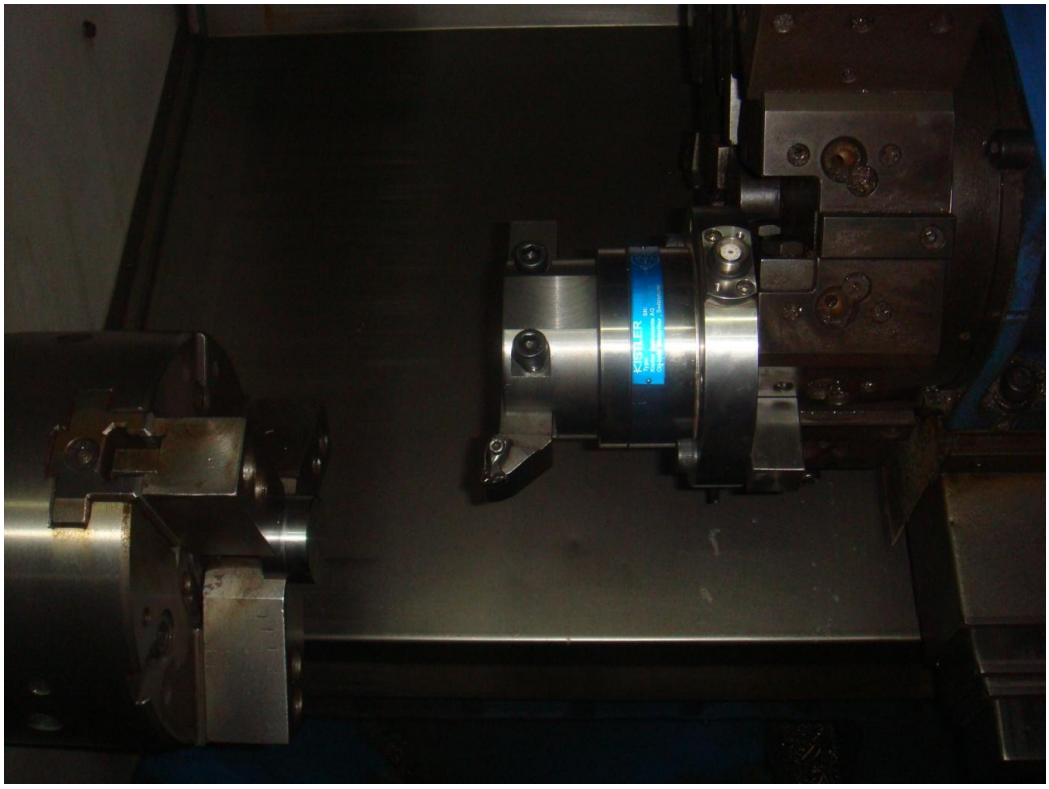

Figure 4.8: Showing tool holder fixture installed on dynamometer installed on turret. Photograph taken on ACE CNC machine.

Figure 4.9: Showing tool holder installed on dynamometer

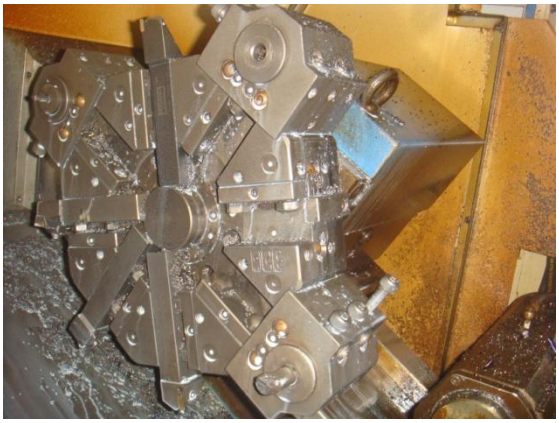

Figure 4.10: Turret of CNC machine

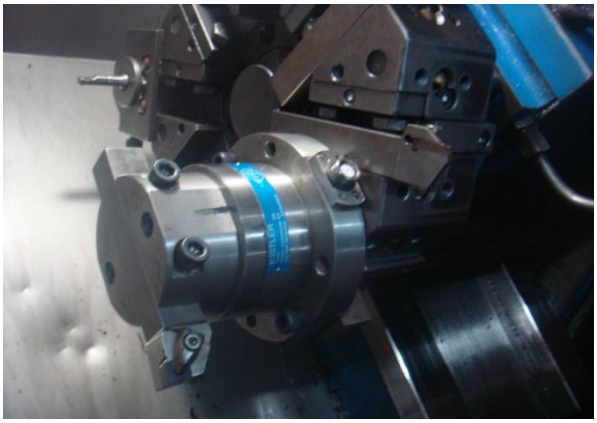

Figure 4.11: Dynamometer setup on M/C

Figure 4.12: Shank to hold dynamometer

Figure 4.13: Tool holder

Figure 4.14: Computer setup

4.7.7 Surface Roughness Calculations

The surface roughness test was done by using Mitutoyo surface roughness tester 'surftest sj 201' was used. The work piece was first clamped on the magnetic v block. Then the probe was adjusted to measure the Ra value. The probe moved a distance of 3 mm.

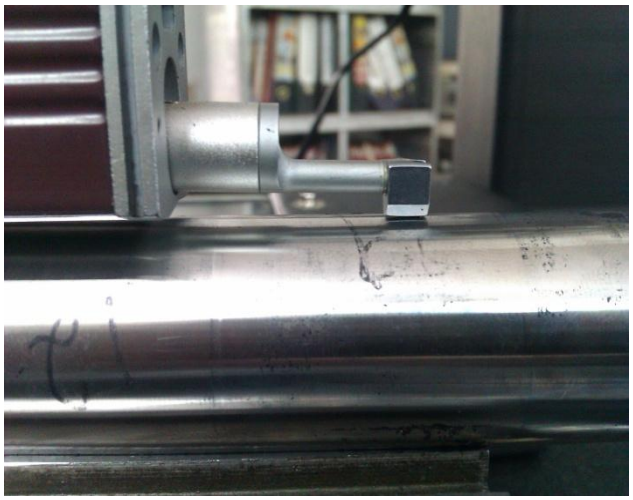

Figure 4.15: Probe of roughness tester

Figure 4.16: Surface roughness setup

4.8 FORCE CALCULATIONS

When we perform the experiment once the cycle start button is pressed on the controller. The turret starts to do its cutting operation. It is that instant when we have to press the "go" button on the dynoware software. In the software the time for which data is to be taken is already set.

After we press the "go" option of the software the amplifier will start recording the forces. The following steps are to be then when the results come

- We get four different graphs showing channel 1, channel 2, channel 3 and channel 4.
- On the keyboard press the "PrtSc" option. And copy this image in MS paint. Save it as a copy
- In the dynoware software go to File , then export the data Select the channels and then press save
- When we save the file it will appear as a notepad file on the location which we have saved.
- Open Microsoft excel and open the notepad file.

- Now we can see an excel file which will show different columns, showing time, forces on channel 1, channel 2, channel 3 and channel 4.
- To calculate the values of the forces. Use the following procedure

  Formulas→more functions→Statistical→Average

  After this a dialog box appears in which we have to enter the cell number and we will receive the average values of the forces in the dialog boxes.

Copy the value of forces from channel 1, channel 2 and channel 3.

On channel 1 we will get value of Radial force F_r

On channel 2 we get value of Feed force F_f

On channel 3 we will get value of Tangential force F_t

For analysis purpose we will be using the machining force F_m which is calculated as.

$$\mathbf{F_m} = \sqrt{\boldsymbol{F_r}^2 + \boldsymbol{F_f}^2 + \boldsymbol{F_t}^2} \qquad \text{----------(Eq. 4.2)}$$

So machining force is used because of some experimental constraints for the complete analysis.

4.9 ANALYSIS OF RESULTS

4.9.1 Signal-to-noise ratio

Parameters that affect the output can be divided in two parts: controllable (or design) factors and uncontrollable (or noise) factors. The value of controllable factors can be adjusted by the designer but the value of uncontrollable factors cannot be changed because they are the sources for variation because of operational environment. The best setting of control factors as they influence the output is determined by performing experiments. There are three possible categories of the response characteristics explained below. [53]

r is the number of tests in a trial (noise of repetitions regardless of noise levels)

MSD = Mean square deviation

y_j= Observed value of the response characteristic

y_o= Nominal or target value of the results

The three different response characteristics are given by the following.

1) **Higher is better**: The S/N for higher the better is given by:

   $(S/N)_{HB}$= -10 log (MSD_{HB})

   Where $MSD_{HB} = \frac{1}{r}\sum_{j=1}^{r}(\frac{1}{y_j{}^2})$ ----------(Eq. 4.3)

   MSD_{HB} = Mean Square Deviation for higher-the-better response.

2) **Nominal is better**: The S/N for nominal is better is:

   $(S/N)_{NB}$= -10 log (MSD_{NB})

   Where $MSD_{NB} = \frac{1}{r}\sum_{j=1}^{r}(y_j - y_o)^2$ ----------(Eq. 4.4)

3) **Lower is better**: In this design situation, the surface roughness, and the machining forces is the type of ‘‘lower is better’’, which is a logarithmic function based on the mean square deviation (MSD), given by

$$S/N_{LB} = -10 \log (MSD) = -10 \log [(\frac{1}{r}\sum_{i=1}^{r} y^2\, i)] \quad \text{----------(Eq. 4.5)}$$

4.9.2 Measurement of F-value of Fisher’s F ratio

The F value determines the significance of the parameters. Larger the F value, the greater the effect on the performance characteristic due to the change in that process parameter. *F* value is defined as:

$$F = \frac{MS\ for\ the\ term}{MS\ for\ the\ error\ term} \quad \text{----------(Eq. 4.6)}$$

4.10 ANOVA

ANOVA is a statistical tool which determines the contribution of individual factors to control the final response. It calculates the parameters like sum of squares (SS_s), degree of freedom, variance, f value, p value for each factor. The ANOVA calculations were done using the help of the MINITAB 15 software. The sum of squares is measure of deviation of the experimental data from the mean value of data. [53]

Let ‘A’ be the factor under investigation.

$$SS_T = \sum_{i=1}^{N}(y_i - \bar{T})^2 \quad \text{----------(Eq. 4.7)}$$

Where N = Number of response observations

$\bar{T}$ is the mean of all observations, y_i is the i^{th} response

Factor Sum of Squares (SS_A) - Squared deviations of factor (A) averages from overall Average

$$SS_A = [\sum_{i=1}^{k_A}(\frac{{A_i}^2}{N_{Ai}})] - \frac{T^2}{N} \quad \text{----------(Eq. 4.8)}$$

Where A_i= Average of all observations under A_i level= A_i / n_{Ai}

T = sum of all observations

$\bar{T}$ = Average of all observations =T/N

n_{Ai} = Number of observations under A_i level

Error Sum of Squares (SS_e) - Squared deviations of observations from factor (A) averages

$$SS_e = \sum_{j=1}^{k_A}\sum_{i=1}^{n_{Ai}}(y_i - \bar{A}_j)^2 \quad \text{----------(Eq. 4.9)}$$

CHAPTER 5

RESULTS AND ANALYSIS

5.1 ANALYSIS OF VARIANCE

The results obtained from the experiment were checked with the help of ANOVA, which predicts the significance of the input parameter for any desired response function. It shows the most significant parameter which influences the results. A confidence interval of 95% has been taken for the analysis.

5.2 ANOVA FOR MACHINING FORCES

Results obtained for the machining forces are shown in the table 5.1 the results for machining forces were obtained from the 27 experiments performed of Taguchi's design with 2 replications. For the analysis purpose the best results are selected. The experimental results analyzed with ANOVA are shown in the table 5.2. The *F* value calculated through MINITAB software is shown in the second last column of ANOVA table which suggests the significance of the factors on the desired characteristics. In the experiment three forces were calculated, the radial force the feed force and the tangential force. From the equation 1 calculate the machining force. Larger is the F value higher is the significance (considering confidence level of 95%). In the table 5.3 ranks have been given to the various factors. Higher is the rank higher is the significance. The results show that feed and hardness are the most significance factor. The combination of nose radius and depth of cut is ranked third After feed, hardness, nose radius-depth of cut, ranked fourth is the cutting speed, which the F test shows has significance; this was because the cutting speed chosen was not in the working range of the ceramic inserts. The different materials have no significant effect on the machining forces.

Table 5.1: Table for machining forces

Hardness HRC	Material	Nose radius - depth of cut(mm)	Cutting speed m/min	Feed mm/rev	Radial force(N)	Tangential force(N)	Feed force(N)	Machining Force(N)
50	EN 31	0.4-0.075	75	0.03	17.317	8.291	2.327	19.339
50	EN 31	0.4-0.075	75	0.06	23.128	9.8856	2.358	25.262
50	EN 31	0.4-0.075	75	0.1	40	17.1	5.641	43.866
50	SAE8620	0.4-0.15	110	0.03	8.158	6.144	0.362	10.219
50	SAE8620	0.4-0.15	110	0.06	15.623	5.797	0.4409	16.669
50	SAE8620	0.4-0.15	110	0.1	50.367	22.93	5.705	55.634
50	EN 9	0.8-0.15	150	0.03	6.649	3.3	1.378	7.549
50	EN 9	0.8-0.15	150	0.06	50.294	23.25	4.614	55.599
50	EN 9	0.8-0.15	150	0.1	21.65	1	2.172	21.781
55	EN 31	0.4-0.15	150	0.03	18.44	6.573	2.0165	19.680
55	EN 31	0.4-0.15	150	0.06	20.063	10.3279	1.65	22.623
55	EN 31	0.4-0.15	150	0.1	65.966	20.209	12.8	70.170
55	SAE8620	0.8-0.15	75	0.03	54.774	26.531	5.506	61.110
55	SAE8620	0.8-0.15	75	0.06	45.3	20.859	5.93	50.223
55	SAE8620	0.8-0.15	75	0.1	48.806	21.279	2.8375	53.318
55	EN 9	0.4-0.075	110	0.03	5.011	3.769	0.8	6.321
55	EN 9	0.4-0.075	110	0.06	10.184	5.011	1.6536	11.469
55	EN 9	0.4-0.075	110	0.1	20.379	7.4784	2.7625	21.882
60	EN 31	0.8-0.15	110	0.03	20.94	8.5315	2.0746	22.706
60	EN 31	0.8-0.15	110	0.06	54.836	25.392	4.633	60.607
60	EN 31	0.8-0.15	110	0.1	80.23	5.567	9.132	80.939
60	SAE8620	0.4-0.075	150	0.03	25.019	10.383	3.678	27.336
60	SAE8620	0.4-0.075	150	0.06	21.937	5.495	1.4955	22.664
60	SAE8620	0.4-0.075	150	0.1	34.24	15.22	3.058	37.594
60	EN 9	0.4-0.15	75	0.03	45.6	23.338	4.5	51.422
60	EN 9	0.4-0.15	75	0.06	63.677	28.018	6.56	69.877
60	EN 9	0.4-0.15	75	0.1	85.302	38.375	9.454	94.012

Table 5.2: Analysis of variance for means of Forces

Source	Degree of freedom	Sum of squares	Variance	F value	Significance
Hardness	2	2627.3	1313.66	5.63	Significant
Material	2	58.9	29.46	0.13	Not- Significant
Nose radius-depth of cut	2	2856.1	1428.03	6.12	Significant
Cutting speed	2	2472.9	1236.44	5.30	Significant
Feed	2	3593.1	1796.55	7.70	Significant
Residual error	16	3731.2	233.20		
Total	26	15339.5			

Table 5.3: Response table for means for forces

Level	Hardness	Material	Depth of cut- Nose radius	Cutting speed	Feed
1	28.44	40.58	23.97	52.05	25.08
2	35.20	37.20	45.59	31.83	37.22
3	51.91	37.77	45.98	31.67	53.24
Delta	23.47	3.38	22.01	20.38	28.17
Rank	2	5	3	4	1

Smaller is better

5.3 MAIN EFFECT PLOTS FOR FORCES:-

Main effect plots for forces are shown in the figure 5.1. Main effect plot shows the variation of forces with respect to hardness, Material type, combined effect of Nose radius and depth of cut, cutting speed and feed. X axis represents change in level of the variable and y axis represents the change in the resultant response. The mean line is shown by the straight horizontal line.

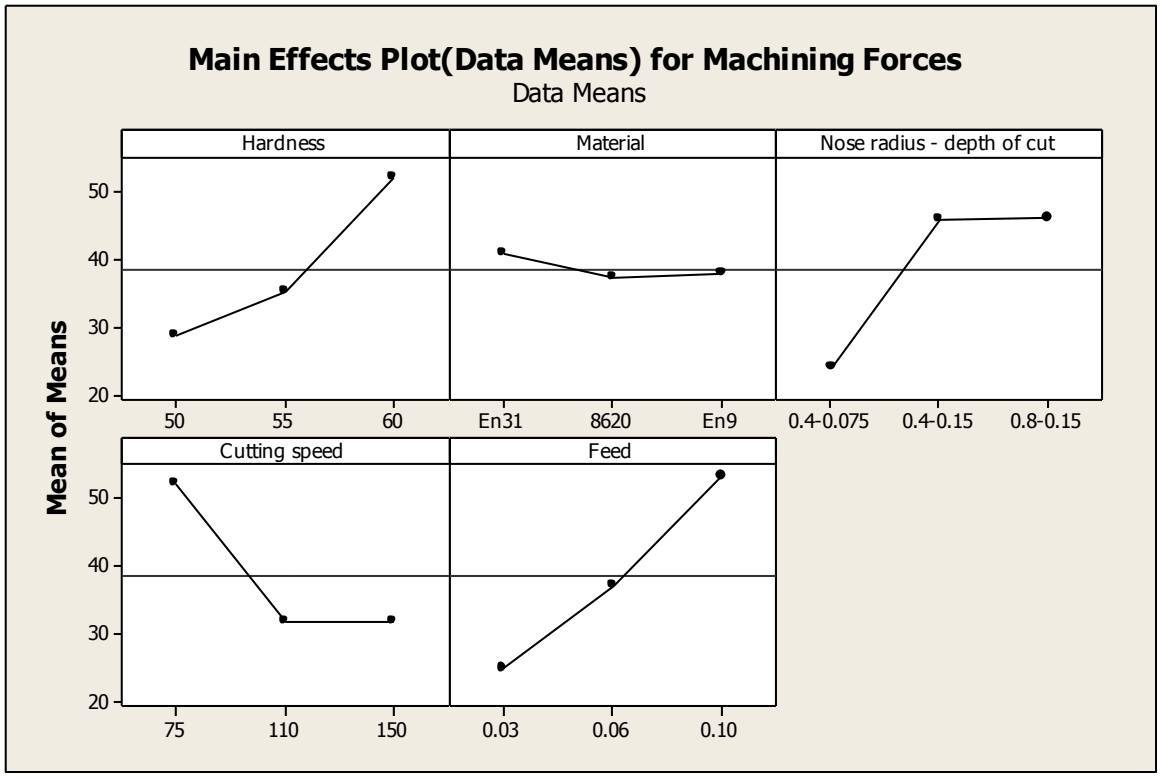

Figure 5.1: Main effects plot for means for machining forces.

5.4 ANALYSIS OF S/N RATIO FOR FORCES:-

The signal to noise ratios tells us about the variations present in the process. The values of all the results according to Taguchi array parameter design layout are presented in this section. The S/N ratios have been calculated to identify the major contributing factors for variation of force values. In this design situation, forces is the type of 'lower is better', which is a logarithmic function based on the mean square deviation (MSD), given by

$$S/N_B = -10 \log(MSD) = -10 \log[(\frac{1}{r}\sum_{i=1}^{r} y^2\, i)] \quad \text{----------(Eq 5.1)}$$

Table 5.4 shows the ANOVA calculations for the S/N ratio. The analysis was carried out at a significance of $\alpha = 0.05$. The main effect is shown in the figure 5.2.Table 5.5 shows the response table for S/N for forces. In the order of significance feed, cutting speed, hardness and nose radius – depth of cut were the most significant factors with F values of 7.58, 5.97, 5.72 and 4.24. Material was not significant factor.

Table 5.4: Analysis of Variance for S/N ratios of Machining forces

Source	Degree of freedom	Sum of Squares	Variance	F	Significant
Hardness	2	197.19	98.60	5.72	Significant
Material	2	35.58	17.79	1.03	Not Significant
Nose radius - depth of cut	2	146.04	73.02	4.24	Significant
Cutting speed	2	205.79	102.90	5.97	Significant
Feed	2	261.34	130.67	7.58	Significant
Residual Error	16	275.65	17.23		
Total	26				

Table 5.5: Response Table for S/N Ratios of Machining forces

Level	Hardness	Material	Depth of cut- Nose radius	Cutting speed	Feed
1	-27.26	-30.83	-26.44	-33.50	-25.69
2	-28.69	-30.13	-31.11	-27.05	-29.93
3	-33.21	-28.20	-31.60	-28.50	-33.54
Delta	5.94	2.63	5.16	6.44	7.86
Rank	3	5	4	2	1

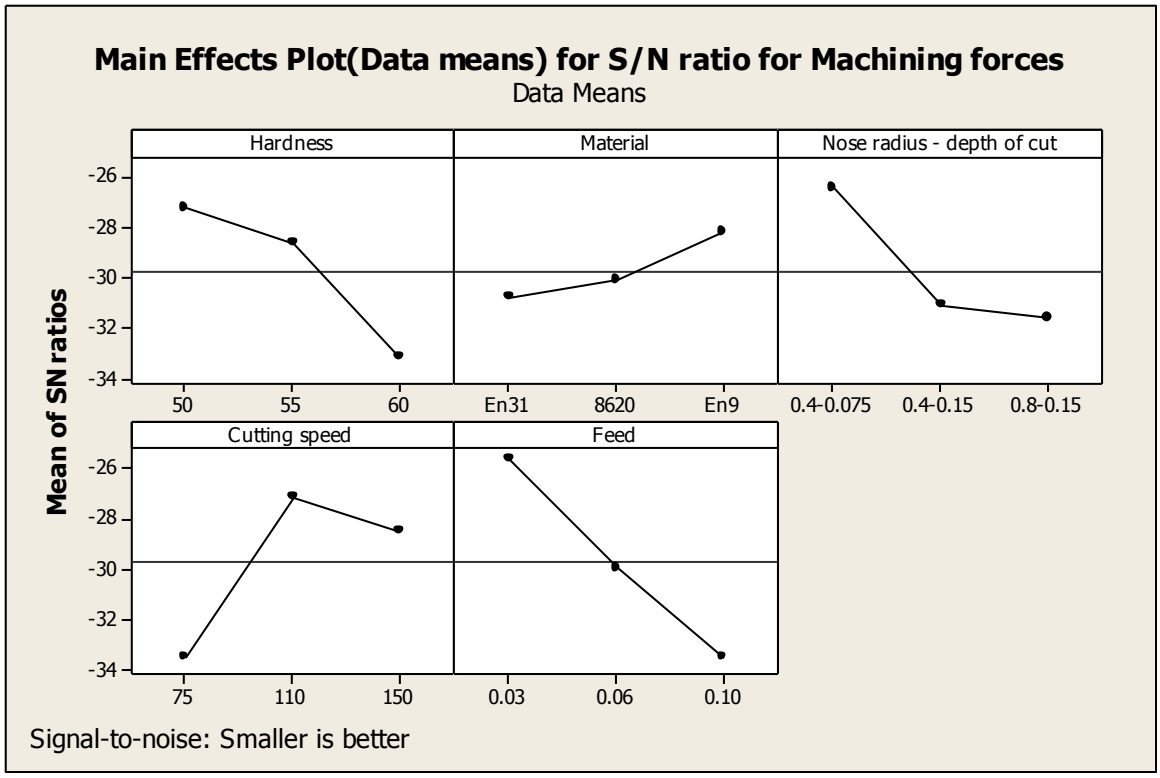

Figure 5.2: Main effects plot for S/N ratios for machining forces

5.5 ANOVA for surface roughness

Results obtained for the surface roughness are shown in the table 5.6. The results for surface roughness were obtained from the 27 experiments performed of Taguchi's design with 2 replications. The experimental results analyzed with ANOVA are shown in the table 5.7. The *F* value calculated through MINITAB software are shown in the second last column of ANOVA table which suggests the significance of the factors on the desired characteristics.. Larger is the F value higher is the significance (considering confidence level of 95%). The results show that only feed is the most significant factor. In the table 5.8 ranks have been given to the various factors. Higher is the rank higher is the significance. Feed is the most significant factor. It should be noted that in two experiments a very rough surface finish was generated, due to experimental constraints those values were not taken and they were assumed respectively to be maximum than other values for the analysis purpose.

Table 5.6: Result for surface roughness.

S.No.	Hardness HRC	Material	Nose radius-depth of cut (mm)	Cutting speed (m/min)	Feed (mm/rev)	Surface Roughness (Ra)
1	50	EN 31	0.4-0.075	75	0.03	0.29
2	50	EN 31	0.4-0.075	75	0.06	0.53
3	50	EN 31	0.4-0.075	75	0.1	0.83
4	50	SAE 8620	0.4-0.15	110	0.03	0.38
5	50	SAE 8620	0.4-0.15	110	0.06	0.97
6	50	SAE 8620	0.4-0.15	110	0.1	1.39
7	50	EN 9	0.8-0.15	150	0.03	0.44
8	50	EN 9	0.8-0.15	150	0.06	1.45*
9	50	EN 9	0.8-0.15	150	0.1	0.79
10	55	EN 31	0.4-0.15	150	0.03	0.31
11	55	EN 31	0.4-0.15	150	0.06	0.75
12	55	EN 31	0.4-0.15	150	0.1	1.09
13	55	SAE 8620	0.8-0.15	75	0.03	0.36
14	55	SAE 8620	0.8-0.15	75	0.06	1.5*
15	55	SAE 8620	0.8-0.15	75	0.1	0.59
16	55	EN 9	0.4-0.075	110	0.03	0.38
17	55	EN 9	0.4-0.075	110	0.06	0.59
18	55	EN 9	0.4-0.075	110	0.1	0.95
19	60	EN 31	0.8-0.15	110	0.03	0.19
20	60	EN 31	0.8-0.15	110	0.06	0.54
21	60	EN 31	0.8-0.15	110	0.1	0.35
22	60	SAE 8620	0.4-0.075	150	0.03	0.42
23	60	SAE 8620	0.4-0.075	150	0.06	0.82
24	60	SAE 8620	0.4-0.075	150	0.1	0.62
25	60	EN 9	0.4-0.15	75	0.03	0.38
26	60	EN 9	0.4-0.15	75	0.06	0.78
27	60	EN 9	0.4-0.15	75	0.1	1.25

* Represents that Very rough surface was generated

Table 5.7: Analysis of variance for means of Surface Roughness (Ra)

Source	Degree of freedom	Sum of Squares	Variance	F	Significance
Hardness	2	0.17147	0.08574	1.11	Not Significant
Material	2	0.34250	0.17125	2.21	Not Significant
Nose radius - depth of cut	2	0.19605	0.09803	1.27	Not Significant
Cutting speed	2	0.05659	0.02829	0.37	Not Significant
Feed	2	1.66805	0.83403	10.77	Significant
Residual Error	16	1.23888	0.07743		
Total	26	3.67354			

Table 5.8: Response table for means for Surface Roughness (Ra)

Level	Hardness	Material	Nose radius-depth of cut	Cutting speed	Feed
1	0.7856	0.5422	0.6033	0.7233	0.3500
2	0.7244	0.7833	0.8111	0.6378	0.8811
3	0.5944	0.7789	0.6900	0.7433	0.8733
Delta	0.1911	0.2411	0.2078	0.1056	0.5311
Rank	4	2	3	5	1

5.6 MAIN EFFECT PLOTS FOR SURFACE ROUGHNESS:-

Main effect plots for surface roughness are shown in the figure 5.3. Main effect plot shows the variation of surface roughness with respect to hardness, Material type, combined effect of Nose radius and depth of cut, cutting speed and feed. X axis represents change in level of the variable and y axis represents the change in the resultant response.

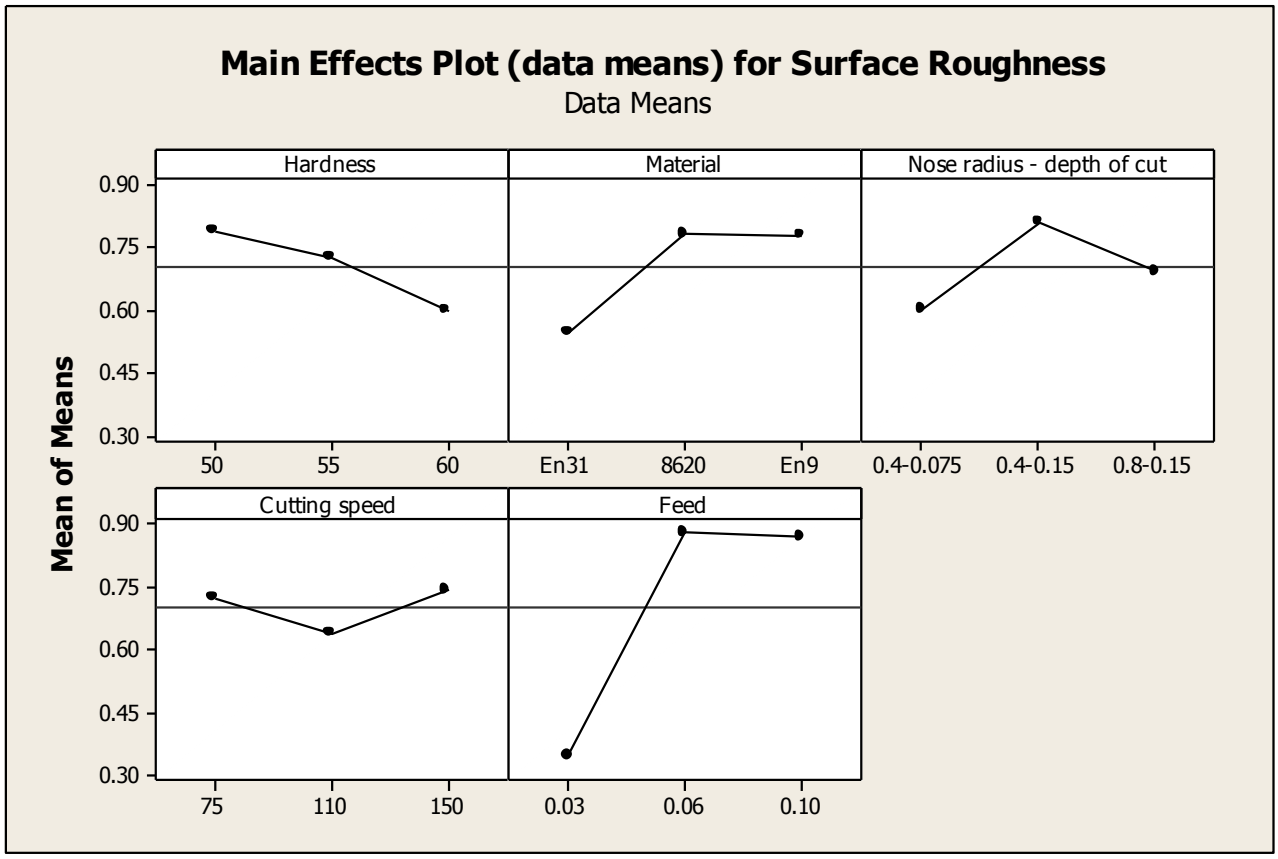

Figure 5.3: Main effects plot for means for surface roughness.

5.7 ANALYSIS OF S/N RATIO FOR SURFACE ROUGHNESS:-

The signal to noise ratios tells us about the variations present in the process. The values of all the results according to Taguchi array parameter design layout are presented in this section. The S/N ratios have been calculated to identify the major contributing factors for variation of force values. In this design situation, forces is the type of 'lower is better', which is a logarithmic function based on the mean square deviation (MSD), given by equation 5.1

$$S/N_B = - 10 \log(MSD) = -10 \log[(\frac{1}{r}\sum_{i=1}^{r} y^2\, i)]$$

Table 5.9 shows the ANOVA calculations for the S/N ratio. The analysis was carried out at a significance of α=0.05. The main effect is shown in the figure 5.4. Table 5.10 shows the

response table for S/N for forces. It was found that only feed and material were a significant factor with F values of 26.23 and 5.12.

Table 5.9: Analysis of variance for S/N ratios for surface roughness (Ra)

Source	Degree of freedom	Sum of Squares	Variance	F test	Significance
Hardness	2	27.02	13.511	2.06	Not Significant
Material	2	67.28	33.642	5.12	Significant
Nose radius - depth of cut	2	25.08	12.539	1.91	Not Significant
Cutting speed	2	16.57	8.284	1.26	Not Significant
Feed	2	344.81	172.405	26.23	Significant
Residual error	16	105.18	6.574		
Total	26	585.94			

Table 5.10: Response table for SN Ratios of surface roughness

Level	Hardness	Material	Nose radius-depth of cut	Cutting speed	Feed
1	3.294	6.523	4.970	4.049	9.345
2	3.921	3.239	2.928	5.349	1.705
3	5.659	3.112	4.976	3.476	1.824
Delta	2.365	3.411	2.047	1.872	7.640
Rank	3	2	4	5	1

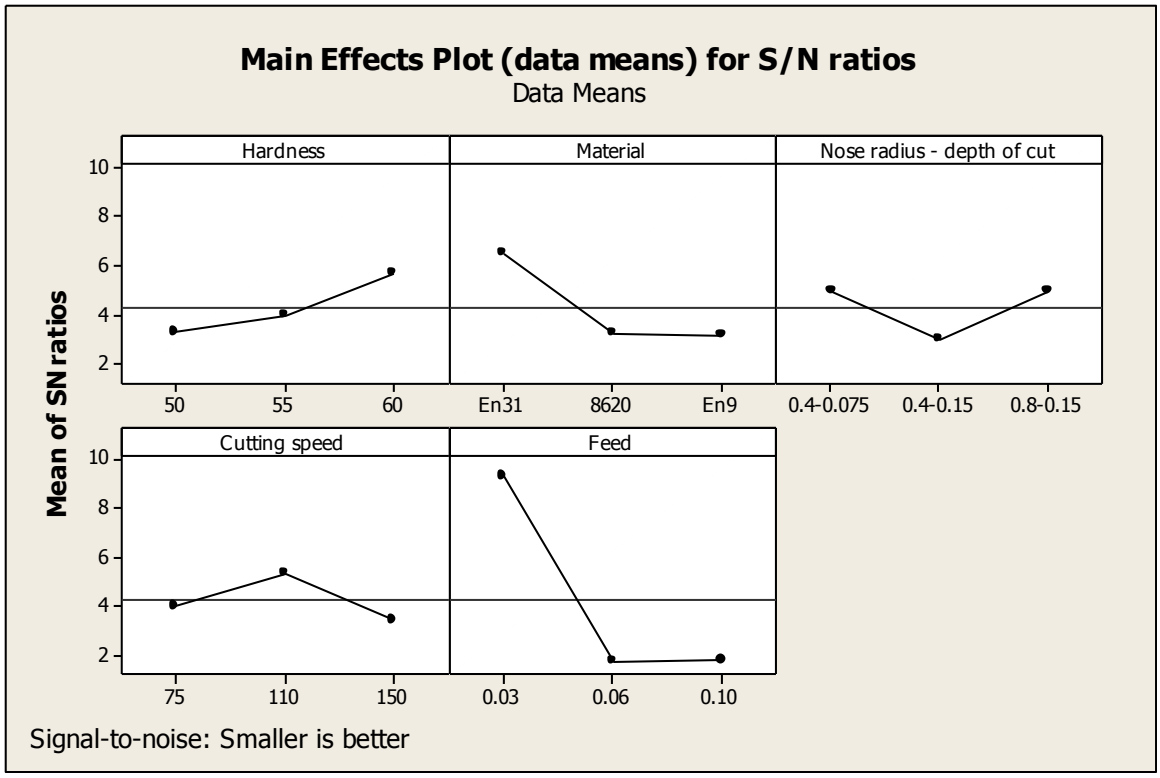

Figure 5.4: Main effects plot for S/N ratios for surface roughness.

5.8 DIMENSIONAL ERROR

The biggest advantage of NC machines is accuracy. They can give dimensional values with tolerance range of ±4 microns. In the turning program exact coordinate setting is to be done to achieve accurate results. So the following steps were done to achieve the required dimensions and to calculate the dimensional error.

1. The program for turning was made and then a trial run was made.
2. After this digital vernier micrometer was used to measure the exact diameter.
3. The diameter reading obtained had some deviation from the desired diameter reading.
4. Offset dimensions were given in the program and then turning was done so that result obtained should be exactly near to the desired value.
5. After this again diameter reading was made with help of digital vernier micrometer.
6. The measured deviation is shown in the table 5.11.

For a shaft of diameter 26 mm if ISO tolerance fit of h6 is applied then a deviation of -16 microns is allowed. So deviation up to 16 microns is acceptable in the shaft

5.9 MATERIAL REMOVAL RATE

Material removal rate is used to determine the amount of material removed per second. It is given by the formula

$$MRR = 1000\ v\ f\ d \qquad \text{---------- (Eq. 5.2)}$$

Where v = cutting speed (m/min)

f = feed (mm/rev)

d = depth of cut (mm)

MRR = material removal rate in mm^3/min.

As the conditions for feed, cutting velocity and depth of cut are fixed so this formula is used to calculate the MRR instead of calculating the initial and the final weight, the above formula was used to calculate the MRR as shown in table 5.12

Table 5.11: Deviation observed from the digital vernier micrometer

Expt no.	Actual diameter (mm)	Required Diameter (mm)	Resultant diameter (mm)	Deviation in microns
1	26.037	25.885	25.896	11
2	26.037	25.885	25.87	15
3	26.037	25.885	25.892	7
4	26.001	25.7	25.715	15
5	26.001	25.7	25.703	3
6	26.001	25.7	25.711	11
7	26.008	25.708	25.705	3
8	26.008	25.708	25.704	4
9	26.008	25.708	25.712	4
10	26	25.7	25.707	7
11	26	25.7	25.714	14
12	26	25.7	25.701	1
13	26.11	25.81	25.816	6
14	26.11	25.81	25.829	19
15	26.11	25.81	25.819	9
16	26	25.85	25.872	12
17	26	25.85	25.851	1
18	26	25.85	25.841	9
19	26.01	25.71	25.701	9
20	25.884	25.584	25.58	4
21	26.01	25.71	25.713	3
22	26	25.85	25.839	11
23	26	25.85	25.864	14
24	26	25.85	25.863	13
25	26.005	25.705	25.7	5
26	26.005	25.705	25.712	7
27	26.005	25.705	25.719	14

Table 5.12: MRR calculated for all the experiments

Hardness	Material	Nose radius - depth of cut (mm)	Cutting speed (m/min)	Feed(mm/rev)	MRR (mm^3/min)
50	EN 31	0.4-0.075	75	0.03	168.75
50	EN 31	0.4-0.075	75	0.06	227.5
50	EN 31	0.4-0.075	75	0.1	562.5
50	SAE 8620	0.4-0.15	110	0.03	495
50	SAE 8620	0.4-0.15	110	0.06	990
50	SAE 8620	0.4-0.15	110	0.1	1650
50	EN 9	0.8-0.15	150	0.03	675
50	EN 9	0.8-0.15	150	0.06	1350
50	EN 9	0.8-0.15	150	0.1	2250
55	EN 31	0.4-0.15	150	0.03	675
55	EN 31	0.4-0.15	150	0.06	1350
55	EN 31	0.4-0.15	150	0.1	2250
55	SAE 8620	0.8-0.15	75	0.03	337.5
55	SAE 8620	0.8-0.15	75	0.06	675
55	SAE 8620	0.8-0.15	75	0.1	1125
55	EN 9	0.4-0.075	110	0.03	247.5
55	EN 9	0.4-0.075	110	0.06	495
55	EN 9	0.4-0.075	110	0.1	825
60	EN 31	0.8-0.15	110	0.03	495
60	EN 31	0.8-0.15	110	0.06	990
60	EN 31	0.8-0.15	110	0.1	1650
60	SAE 8620	0.4-0.075	150	0.03	337.5
60	SAE 8620	0.4-0.075	150	0.06	675
60	SAE 8620	0.4-0.075	150	0.1	1125
60	EN 9	0.4-0.15	75	0.03	337.5
60	EN 9	0.4-0.15	75	0.06	675
60	EN9	0.4-0.15	75	0.1	1125

5.10 DETERMINATION OF OPTIMUM SOLUTION USING GREY RELATIONAL ANALYSIS

The grey relational analysis is used to convert multi response process optimization problem in to single response optimization problem and then grey relational grade is determined. The objective is to maximise the grey relational grade and determine the optimal combination. Following steps are used to calculate the grey relational grade

1. **Calculation of pre processed data result**:- For lower the better characteristic following equation is to be used to calculate the data

$$x_i(k)=\frac{y_i(k)-\min y_i(k)}{\max y_i(k)-\min y_i(k)} \qquad \text{----------(Eq 5.3)}$$

For higher the better characteristic following equation is to be used to calculate data

$$x_i(k)=\frac{\max y_i(k)-y_i(k)}{\max y_i(k)-\min y_i(k)} \qquad \text{----------(Eq 5.4)}$$

Where $x_i(k)$ is the value after grey relational generation, min $y_i(k)$ is smallest value of $y_i(k)$ for the k^{th} response, and max $y_i(k)$ is largest value of $y_i(k)$ for the k^{th} response. The data is calculated in table 5.13

2. **Calculation of Grey relational coefficient** :- The grey relational coefficient is calculated in table 5.14 by the following relation

$$\xi(x_{0j},x_{ij}) = \frac{\Delta_{min}+\zeta\,\Delta_{max}}{\Delta_{ij}+\zeta\Delta_{max}} \qquad \text{----------(Eq 5.5)}$$

$\Delta_{ij} = I x_{0j} - x_{ij} I$

Δ_{min} = Min $\{\Delta_{ij}$, i= 1, 2,....., m; j = 1,2,.....n$\}$,

Δ_{max} = Max $\{\Delta_{ij}$, i= 1, 2,....., m; j = 1,2,.....n$\}$,

ζ is the distinguishing coefficient and its value is usually taken as 0.5.

3. **Calculation of grey relational grade**: - Find the average of all individual response coefficients by following relation as calculated in table 5.15

$$\gamma\,(x_{0j},x_{ij}) = \frac{1}{n}\sum_{k=1}^{n}\xi(x_{oj},x_{ij}) \qquad \text{----------(Eq 5.6)}$$

4. **Response table for grey relational grade**: - The response table is made for every factor. This is done by adding the grey relational grades value for the factors as done in table 5.16. For example to determine the mean of grey relational grades for

hardness at level 1, level 2 and level 3. Find the mean of grey relational grades for values 1-9, 10 -18, 19 -27 correspondingly. [54]

Table 5.13: Preprocessed data obtained from experimental values.

Experimental data					Preprocessed data			
S.No	**Machining forces N**	**Surface roughness Ra**	**Deviation in microns**	**MRR mm^3/min**	**mf**	**Sr**	**dd**	**Mrr**
1	19.34	0.29	11	168.75	0.1484	0.07633	0.5556	1
2	25.28	0.53	15	227.5	0.2162	0.2595	0.7778	0.9717
3	43.86	0.83	7	562.5	0.4280	0.4885	0.3333	0.8108
4	10.21	0.38	15	495	0.0443	0.1450	0.7778	0.8432
5	12.57	0.97	3	990	0.0712	0.5954	0.1111	0.6054
6	55.6	1.39	11	1650	0.5619	0.9160	0.5556	0.2883
7	7.55	0.44	3	675	0.0140	0.1908	0.1111	0.7567
8	55.64	1.45	4	1350	0.5624	0.9618	0.1667	0.4324
9	21.8	0.79	4	2250	0.1765	0.458	0.1667	0
10	19.68	0.31	7	675	0.1524	0.0916	0.3333	0.7567
11	22.664	0.75	14	1350	0.1863	0.4274	0.7222	0.4324
12	70.18	1.09	1	2250	0.7282	0.687	0	0
13	61.03	0.36	6	337.5	0.6239	0.1297	0.2778	0.9189
14	50.11	1.5	19	675	0.4993	1	1	0.7567
15	53.31	0.59	9	1125	0.5358	0.3053	0.4444	0.5405
16	6.32	0.38	12	247.5	0	0.1450	0.6111	0.9621
17	11.47	0.59	1	495	0.0587	0.3053	0	0.8432
18	21.79	0.95	9	825	0.1764	0.5801	0.4444	0.6846
19	22.7	0.19	9	495	0.1867	0	0.4444	0.8432
20	70.8	0.54	4	990	0.7353	0.2671	0.1667	0.6054
21	83.24	0.35	3	1650	0.8771	0.1221	0.1111	0.2882
22	27.37	0.42	11	337.5	0.24	0.1755	0.5556	0.9189
23	22.664	0.82	14	675	0.1863	0.4809	0.7222	0.7567
24	37.59	0.62	13	1125	0.3565	0.3282	0.6667	0.5405
25	51.866	0.38	5	337.5	0.5193	0.145	0.2222	0.9189
26	69.6	0.78	7	675	0.7216	0.4503	0.3333	0.7567
27	94.01	1.25	14	1125	1	0.8091	0.7222	0.5405

Table 5.14: Determination of Grey relational coefficient

Preprocessed data				Grey relational coefficient			
Mf	**Sr**	**Dd**	**mrr**	**ξ mf**	**ξ sr**	**ξ dd**	**ξ mrr**
0.1484	0.07633	0.5556	1	0.6981	0.8675	0.4736	0.3333
0.2162	0.2595	0.7778	0.9717	0.7710	0.6582	0.3913	0.3397
0.4280	0.4885	0.3333	0.8108	0.5387	0.5057	0.6	0.3814
0.0443	0.1450	0.7778	0.8432	0.9185	0.7751	0.3913	0.3722
0.0712	0.5954	0.1111	0.6054	0.8752	0.4564	0.8181	0.4523
0.5619	0.9160	0.5556	0.2883	0.4708	0.3531	0.4736	0.6342
0.0140	0.1908	0.1111	0.7567	0.9727	0.7237	0.8181	0.3978
0.5624	0.9618	0.1667	0.4324	0.4706	0.342	0.75	0.5362
0.1765	0.458	0.1667	0	0.739	0.5219	0.75	1
0.1524	0.0916	0.3333	0.7567	0.7664	0.8451	0.6	0.3978
0.1863	0.4274	0.7222	0.4324	0.7284	0.539	0.40909	0.5362
0.7282	0.687	0	0	0.407	0.4212	1	1
0.6239	0.1297	0.2778	0.9189	0.4448	0.7939	0.6428	0.3523
0.4993	1	1	0.7567	0.5003	0.3333	0.3333	0.3978
0.5358	0.3053	0.4444	0.5405	0.4826	0.6208	0.5294	0.4805
0	0.1450	0.6111	0.9621	1	0.7751	0.45	0.3419
0.0587	0.3053	0	0.8432	0.8948	0.6208	1	0.3722
0.1764	0.5801	0.4444	0.6846	0.7392	0.4628	0.5294	0.422
0.1867	0	0.4444	0.8432	0.728	1	0.5294	0.3722
0.7353	0.2671	0.1667	0.6054	0.4047	0.6517	0.75	0.4523
0.8771	0.1221	0.1111	0.2882	0.363	0.8036	0.81818	0.6342
0.24	0.1755	0.5556	0.9189	0.6756	0.7401	0.4736	0.3523
0.1863	0.4809	0.7222	0.7567	0.7284	0.5097	0.40909	0.3978
0.3565	0.3282	0.6667	0.5405	0.5837	0.6036	0.42857	0.4805
0.5193	0.145	0.2222	0.9189	0.4904	0.7751	0.6923	0.3523
0.7216	0.4503	0.3333	0.7567	0.4093	0.5261	0.6	0.3978
1	0.8091	0.7222	0.5405	0.3333	0.3819	0.40909	0.4805

Table 5.15: Calculation of Grey relational grade

ξ mf	ξ sr	ξ dd	ξ mrr	grey relational grade γ
0.7710	0.8675	0.4736	0.3333	0.611
0.6981	0.6582	0.3913	0.3397	0.521
0.5387	0.5057	0.6	0.3814	0.5064
0.9185	0.7751	0.3913	0.3722	0.6143
0.8752	0.4564	0.8181	0.4523	0.6505
0.4708	0.3531	0.4736	0.6342	0.4829
0.9727	0.7237	0.8181	0.3978	0.7281
0.4706	0.342	0.75	0.5362	0.5247
0.739	0.5219	0.75	1	0.7527
0.7664	0.8451	0.6	0.3978	0.6524
0.7284	0.539	0.40909	0.5362	0.5532
0.407	0.4212	1	1	0.707
0.4448	0.7939	0.6428	0.3523	0.5585
0.5003	0.3333	0.3333	0.3978	0.3912
0.4826	0.6208	0.5294	0.4805	0.5283
1	0.7751	0.45	0.3419	0.6417
0.8948	0.6208	1	0.3722	0.7219
0.7392	0.4628	0.5294	0.422	0.5384
0.728	1	0.5294	0.3722	0.6575
0.4047	0.6517	0.75	0.4523	0.5647
0.363	0.8036	0.81818	0.6342	0.6548
0.6756	0.7401	0.4736	0.3523	0.5604
0.7284	0.5097	0.40909	0.3978	0.5113
0.5837	0.6036	0.42857	0.4805	0.5241
0.4904	0.7751	0.6923	0.3523	0.5776
0.4093	0.5261	0.6	0.3978	0.4833
0.3333	0.3819	0.40909	0.4805	0.4012

The optimal solution is found by the following table 5.16

Table 5.16: Optimum conditions table

	level 1	**level 2**	**level 3**	**Max-Min**
Hardness	**5.3932**	5.2929	4.9348	.4584
Material	4.9228	4.8217	**5.3698**	.5481
Nose radius-DOC	5.1377	5.1225	**5.3606**	.2381
Cutting Speed	4.5799	**5.6407**	5.5141	1.0608
Feed	**5.5837**	4.9410	5.0961	.6427

From the following table the optimal conditions determined are

A - Hardness – 50 RC

B - Material - EN 9

C - Nose radius- 0.8 mm

Depth of cut – .15 mm

D - Cutting speed – 110 m/min

E- Feed – 0.03 mm/rev

The optimal combination is

$\mathbf{A_1B_3C_3D_2E_1}$

But hardness and material are dependent on the requirements of the process. So hardness and material can be chosen as per the systems configuration. Therefore the $\mathbf{A_{1\text{-}3}B_{1\text{-}3}C_3D_2E_1}$ is the most optimum combination.

5.11 GENETIC PROGRAMMING

Genetic programming is an evolutionary based methodology for creating computer programs to do user defined functions. The evolutionary search is based on Darwinian principle of natural selection (survival of the fittest) and it is analogy to the various biological processes like crossover, mutation, gene duplication and gene deletion.

Genetic programming achieves this goal of automatic programming by genetically breeding population of computer programs. For genetic programming to be done following steps are, to be used by the human user to specify the problem:-

1. The set of terminals (e.g. the independent variables of the problem)
2. The set of primitive functions
3. The fitness measure
4. The parameters used for controlling the run
5. The result of the run [57]

Genetic algorithm is started with set of solutions (chromosomes) called population. Solutions from one problem are taken and are used to form a new population. Solutions, which are selected to form new solutions, are selected according to their fitness. The more fit they are the more chances they have to reproduce and likewise the best results are obtained.

Outline of Basic genetic Algorithm:-

1. [Start] Generate random population of n chromosomes.
2. [Fitness] Evaluate the fitness of each chromosome x in the population.
3. [New population] population is generated in analogy to biological processes with the following steps
    - [Selection] Select two parent chromosomes.
    - [Crossover] Crossover the parents to form a new offspring.
    - [Mutation] Mutate new offspring at each position.
    - [Accepting] Place new offspring in new population.
4. [Replace] Use new generated population for further run.
5. [Test] If end condition is satisfied stop and return the best solution.
6. Go to Step 2 [58,59]

To find the optimal solution using Genetic Algorithm, Multiobjective Genetic Algorithm Solver a subroutine of Global Optimization Toolbox [60] used. Global Optimization Toolbox

solvers are designed to search through more than one basin of attraction. They search in various ways like Genetic Algorithm (ga), simulannealbnd, patternsearch, GlobalSearch and MultiStart. We had used gamultiobj solver search method as it uses a set of starting points (called the population) and iteratively generates better points from the population. As long as the initial population covers several basins, gamultiobj examines several basins to find the best fit. This procedure enables the software to find the minima of multiple functions.

The gamultiobj solver uses a controlled elitist genetic algorithm (a variant of NSGA-II [60]). An elitist GA always favours individuals with better fitness value (rank). A controlled elitist GA also favours individuals that can help increase the diversity of the population even if they have a lower fitness value. It is important to maintain the diversity of population for convergence to an optimal Pareto front. Diversity is maintained by controlling the elite members of the population as the algorithm progresses. Two options, ParetoFraction and DistanceFcn, control the elitism. ParetoFraction limits the number of individuals on the Pareto front (elite members). The distance function, selected by DistanceFcn, helps to maintain diversity on a front by favouring individuals that are relatively far away on the front.

To run the solver, multiple objective functions defined using the set of experimental data. Each objective function is a mathematical linear relationship between independent (taken as decision variables i.e. x_j, $j = 1\ to 5$) and dependent variables (variables needs to optimised). The linear relationship for each dependent variable (z_i, $i = 1\ to\ 4$) defined by regression lines and describe as follows for the study.

$$z_1 = 0.946 - 0.0191x_1 + 0.00032x_2 + 7.06x_3 + 0.118x_4 + 0.0433x_5;$$

$$z_2 = -(-820 - 10.7x_1 + 8.08x_2 + 13975x_3 - 21.6x_4 + 271x_5);$$

$$z_3 = 13.5 + 0.078x_1 - 0.0316x_2 - 13.5x_3 - 0.67x_4 - 1.78x_5;$$

$$z_4 = -106 + 2.35x_1 - 0.265x_2 + 402x_3 - 1.40x_4 + 11.0x_5;$$

Here,

z_1: Surface finish

z_2: Material Removal rate

z_3: Dimensional deviation

z_4: Machining Forces

where as x_1 : Hardness

x_2 : Cutting speed

x_3 : Feed rate

x_4 : The material EN 31, EN 9 and SAE 8620

x_5 : This is combination of nose radius and depth of cut, 0.04-0.075, 0.04 – 0.15, 0.8-0.15.

Our objective is to minimise each function defined above under the following restrictions on variables

$50 \le x_1 \le 60,\ 75 \le x_2 \le 150,\ 0.03 \le x_3 \le 0.10,$

x_4 : To generate regression equation values taken were 1, 2 and 3,

x_5 : To generate regression equation values taken were 1, 2 and 3

The above stated problem defined in a fit.m file to run the solver and shown in figure 1

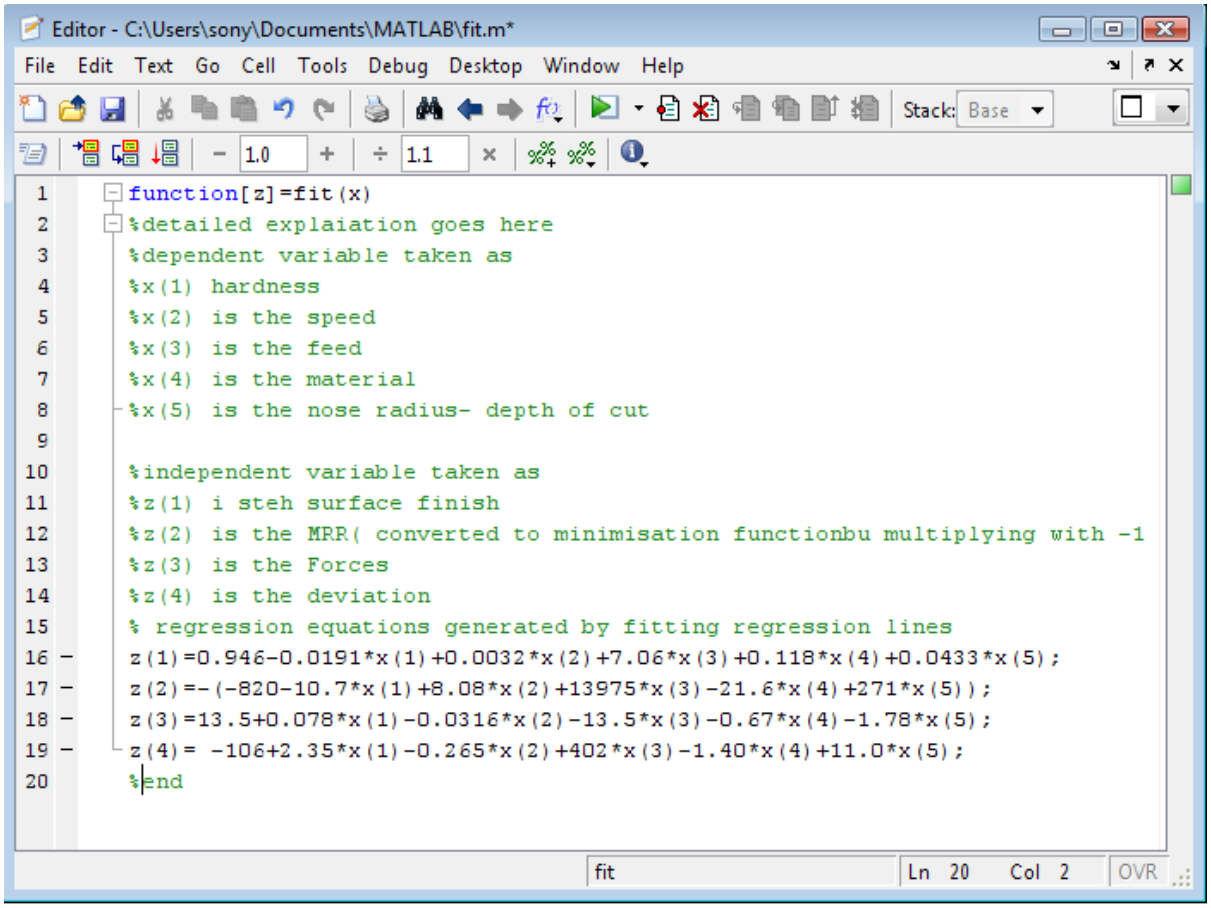

Figure 5.5: fit.m file to run solver

Table 5.17: Output generated by Genetic Algorithm

S.no	Hardness X(1)	Speed X(2)	Feed X(3)	Material X(4)	Nose Radius-depth of cut X(5)	surface finish z(1)	Dimensional Deviation Z(3)	Machining Forces Z(4)	Material removal rate Z(2)
1	60	147	0.03	EN 31	0.4-0.075	0.22	10.67	17.63	396
2	53	106	0.03	SAE 8620	0.4-0.075	0.41	11.02	13.22	149
3	53	110	0.03	SAE 8620	0.4-0.075	0.42	10.73	11.91	203
4	54	115	0.04	SAE 8620	0.4-0.075	0.43	10.65	14.90	304
5	60	150	0.05	EN31	0.8-0.15	0.44	6.77	46.57	1226
6	51	133	0.04	SAE 8620	0.4-0.075	0.5	9.81	3.44	441
7	50	139	0.03	SAE 8620	0.4-0.075	0.51	9.49	-0.87	487
8	50	146	0.03	SAE 8620	0.4-0.075	0.53	9.27	-4.09	537
9	50	148	0.03	SAE 8620	0.4-0.075	0.53	9.19	-5.61	541
10	50	147	0.04	SAE 8620	0.4-0.075	0.55	9.05	-3.16	607
11	50	142	0.04	SAE 8620	0.4-0.075	0.59	9.26	-0.59	611
12	50	144	0.04	SAE 8620	0.4-0.075	0.59	9.22	-1.89	617
13	60	150	0.07	EN 31	0.8-0.15	0.61	6.43	56.49	1571
14	53	122	0.05	SAE 8620	0.4-0.075	0.61	9.50	19.99	670
15	52	124	0.06	SAE 8620	0.4-0.075	0.65	9.48	17.96	689
16	51	138	0.05	SAE 8620	0.4-0.075	0.66	8.56	8.80	753
17	51	137	0.05	SAE 8620	0.4-0.075	0.67	8.59	9.60	765
18	50	150	0.04	EN 9	0.4-0.075	0.71	8.34	-5.61	613
19	50	143	0.05	SAE 8620	0.4-0.075	0.72	7.95	9.67	908
20	52	115	0.07	EN 9	0.4-0.15	0.85	8.03	30.62	965
21	53	112	0.07	SAE 8620	0.4-0.15	0.86	7.93	36.45	1016
22	54	125	0.08	SAE 8620	0.8-0.15	0.88	6.72	45.61	1377
23	53	109	0.07	SAE 8620	0.4-0.15	0.89	7.63	38.49	1019
24	52	106	0.08	SAE 8620	0.4-0.15	0.89	8.00	38.51	1031
25	54	118	0.08	SAE 8620	0.8-0.15	0.90	6.44	49.90	1369
26	54	121	0.08	SAE 8620	0.4-0.15	0.91	7.29	41.24	1253
27	55	125	0.10	SAE 8620	0.8-0.15	0.95	6.50	56.83	1634
28	53	127	0.08	EN 9	0.4-0.15	0.96	6.67	38.81	1348
29	52	137	0.08	EN 9	0.8-0.15	0.97	5.62	34.96	1444
30	54	140	0.10	SAE 8620	0.8-0.15	0.99	5.45	53.59	1829
31	53	125	0.09	SAE 8620	0.8-0.15	1.00	6.20	49.53	1572
32	54	141	0.10	SAE 8620	0.8-0.15	1.02	5.25	51.90	1851
33	53	118	0.09	EN 9	0.4-0.15	1.04	6.36	48.74	1465
34	51	146	0.08	EN 9	0.8-0.15	1.06	4.71	37.15	1693
35	51	138	0.1	EN 9	0.8-0.15	1.13	5.30	42.02	1733
36	51	138	0.1	EN 9	0.8-0.15	1.13	5.29	42.11	1735
37	50	150	0.1	EN 9	0.4-0.075	1.16	6.97	22.14	1544
38	51	138	0.1	EN 9	0.8-0.15	1.16	5.22	43.67	1790
39	51	148	0.1	EN 9	0.8-0.15	1.19	4.24	43.49	1962
40	50	150	0.1	EN 9	0.8-0.15	1.20	4.96	34.58	1850
41	50	150	0.1	EN 9	0.8-0.15	1.22	4.40	38.04	1935
42	50	150	0.1	EN 9	0.8-0.15	1.22	4.22	39.12	1962

42 solutions were obtained by using genetic algorithm approach and six best solutions from this table were selected under the conditions. But in this table the criterion to select the best solution depends on the user. In the first six outputs obtained, it was found that the surface finish obtained was the best so these can be selected. Moreover after experiment seven the surface finish began to deteriorate, also the forces obtained were in negative which is not possible. So the outputs seven to twelve cannot be accepted. Other optimum combinations depend on the type of requirement of the user. If tool wear is to be minimized than the combination selected can be the one which consumes least force. If productivity is to be increased than we can select the optimum condition for higher material removal rate. If both forces are to be minimized and best quality is to be obtained than we have to select the first combination. Dimensional deviation was under 10 microns so that is acceptable in all cases because of the tolerance range h6 for shafts.

CHAPTER 6

METALLURGICAL ANALYSIS

6.1 METALLURGICAL ANALYSIS

In this analysis a study was made to understand the phase transformations using XRD machine. The white layer formation was studied using Leica microscopy and SEM was used to find the turning pattern generated by grinded sample and hard turned sample. Micro stress and the crystallite size was also calculated using Devy Scherrer equation. The following samples shown in table 6.1 were selected for the metallurgical analysis. To make a comparison three virgin samples were taken on which no hardening was done and one centreless grinded sample of SAE 8620 was taken.

Table 6.1: Samples selected for analysis

Sample number	Hardness(HRC)	Material	Nose radius – depth of cut (mm)	Cutting speed (m/min)	Feed (mm/rev)
34	50	EN 9	0.8-0.15	150	0.03
37	55	EN 31	0.4-0.15	150	0.03
46	60	EN 31	0.8-0.15	110	0.03
49	60	8620	0.4-0.075	150	0.03
52	60	EN 9	0.4-0.15	75	0.03
Virgin sample of EN 31					
Virgin sample of EN 9					
Virgin sample of SAE 8620					
Grinded sample of SAE 8620 (60 HRC)					

6.2 XRD

Xray Diffraction is a technique used for phase identification of different materials. It works on the principal that there is a cathode which emits the electrons. The electrons are accelerated with the applied voltage and the electrons strike the target material. The electrons have high energy to penetrate into the target material. When they strike the material spectra is produced which comprises of several components, mainly being K_α and K_β. Copper material was used in the Pan analytical system machine as a target material with Cu K_α radiation = 1.5418Å. The X rays are focussed to the sample. The sample and the detector are rotated and the intensity of reflected rays is recorded. The detector converts the X ray signal into a count rate which is generate don the output screen. The path of the focussed X ray is at an angle θ while X ray detector which is mounted on an arm rotates at an angle 2θ. Data is collected at 2θ angle. [55]

Applications of XRD

1. Identification of unknown crystalline materials.
2. Characterization of crystal materials
3. Determination of crystal lattice size
4. To measure purity of sample.

Machine used: - X'PERT PRO of PAN ANALYTICAL using CuKα radiation

Software for generating data: PAN ANAYTICAL SYSTEM

Sample preparation: On the XRD machine a standard dimension specimen can only be placed. The sample of the size 10 X 10 X 2 mm was required, where 2 mm is the thickness. The sample was parted carefully on the surface grinder machine with the help of parting wheel. Care was taken so that the turned layer does not get damaged. 8 samples were selected for this purpose. The main purpose of XRD was to determine the phase changes after hard turning at different hardness and before hardening (virgin sample).

Peaks obtained were matched using the Pc PDF software which had cards to match the peak data.

6.3 RESULTS OBTAINED FROM X-RAY DIFFRACTION ANALYSIS

X-ray diffraction of different samples was carried out by X'PERT PRO of PAN ANALYTICAL using CuKα radiation. In XRD, the physical content of the constituents present in the samples are indicated in the form of a graphs and tables shows the name and percentage of element/ compound present in respective Samples.

Sample EN 31: Virgin sample turned without hardening

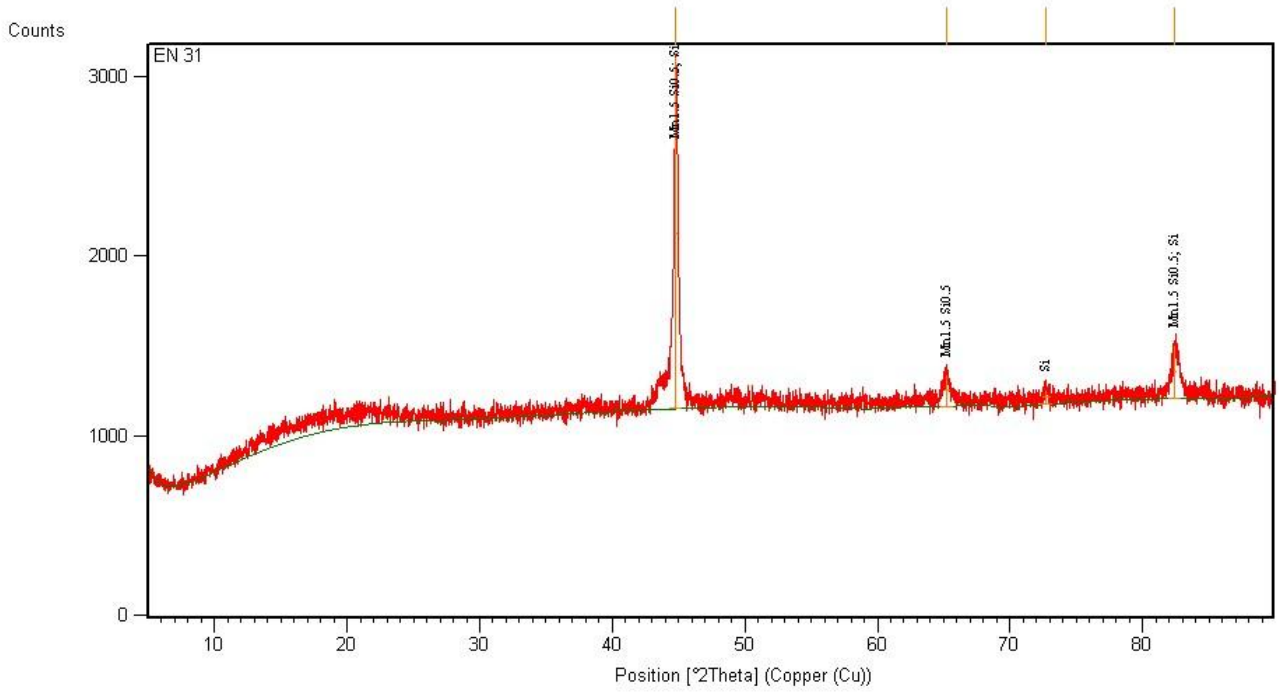

Figure 6.1: Peaks obtained for virgin sample EN 31

Table 6.2: XRD results of virgin sample EN 31

Ref.Code	Score	Compound Name	Scale Factor	Chemical Formula	Weight fraction (%)
01-074-6696	83	Manganese Silicide	0.747	$Mn_{1.5}$ $Si_{0.5}$	27.0
01-089-9056	19	Silicon	0.268	Si	73.0

Table number 6.2 shows the X-ray diffraction pattern of EN 31 (virgin sample), which show the presence of manganese silicide and Silicon .

In X-ray diffraction (figure number 6.1), Four peaks have been obtained in the 2θ span ranging from 10 to 90. From these peaks the maximum value of relative intensity [%] is 100.00 at the position [^{0}2Th.] of 44.7964 gives two assignments i.e. $Mn_{1.5}$ $Si_{0.5}$ and Si. The peaks in the pattern can be indexed to a mixture of different alloying elements and other remaining minor peaks attributed to impurity.

Sample number 46: Hardened to 60 HRC and turned

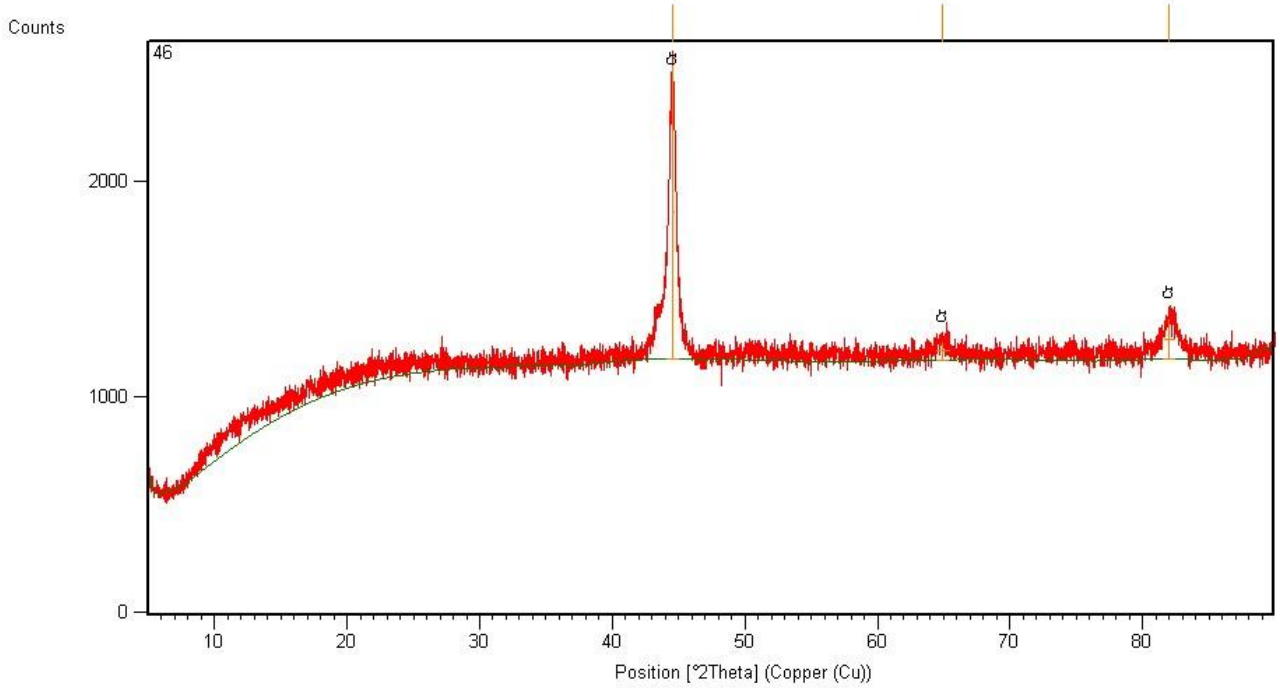

Figure 6.2: Peaks obtained for sample number 46

Table 6.3: XRD results of sample 46

Ref.Code	Score	Compound Name	Scale Factor	Chemical Formula	Weight fraction (%)
00-006-0694	70	Chromium	0.873	Cr	100.0

In X-ray diffraction (figure number 6.2), Three peaks have been obtained in the 2θ span ranging from 10 to 90. From these peaks the maximum value of relative intensity [%] is 90.00 at the position [^{0}2Th.] of 44.5402 gives one assignment i.e. Cr.

After turning of EN 31 at 60 HRC it was found that the manganese silicide phase disappeared and only chromium was found.

Sample EN 9: turned without hardening

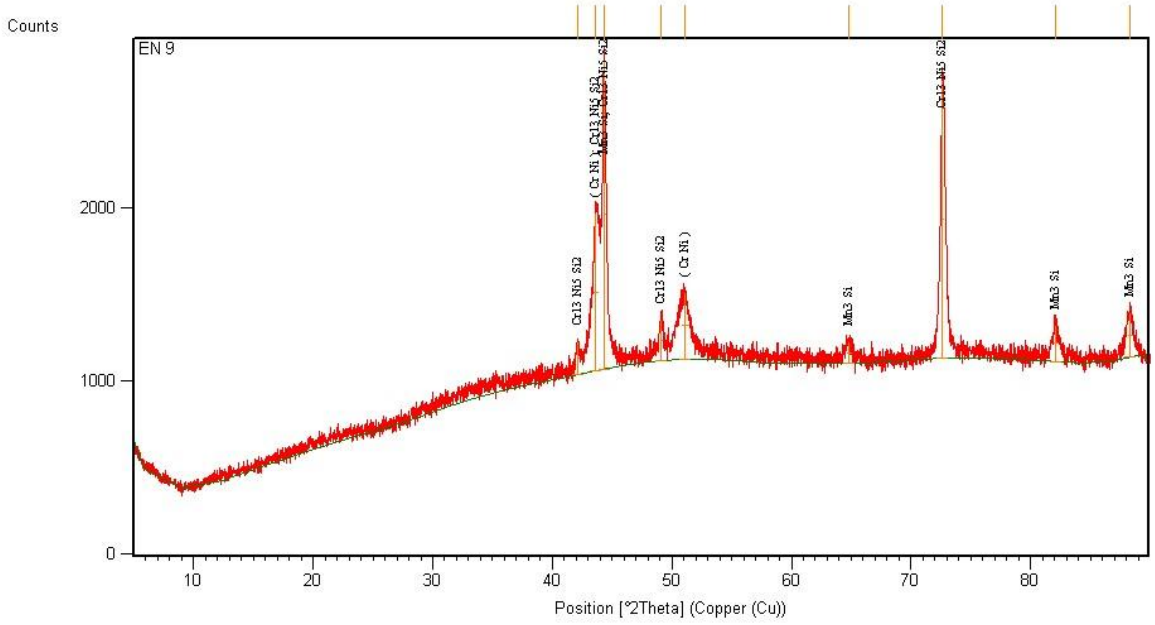

Figure 6.3: Peaks obtained for virgin sample EN 9

Table 6.4: XRD results of EN 9

Ref.Code	Score	Compound Name	Scale Factor	Chemical Formula	Weight fraction (%)
03-065-6979	57	Manganese Silicide	0.903	Mn_3 Si	3.0
01-071-7594	52	Chromium Nickel	0.469	Cr Ni	2.0
00-054-0370	29	Chromium Nickel Silicon	0.899	Cr_{13} Ni_5 Si_2	95.0

Table number 6.4 shows the X-ray diffraction pattern of EN 9 (virgin sample), which show the presence of Manganese Silicide, Chromium Nickel and Chromium Nickel Silicon.

In X-ray diffraction (figure number 6.3), Nine peaks have been obtained in the 2θ span ranging from 10 to 90. From these peaks the maximum value of relative intensity [%] is 100.00 at the position [^{0}2Th.] of 44.3137 gives two assignments i.e. Mn_3 Si and Cr Ni. The peaks in the pattern can be indexed to a mixture of different alloying elements and other remaining minor peaks attributed to impurity.

Sample number 52: **At 60 HRC after hard turning EN 9**

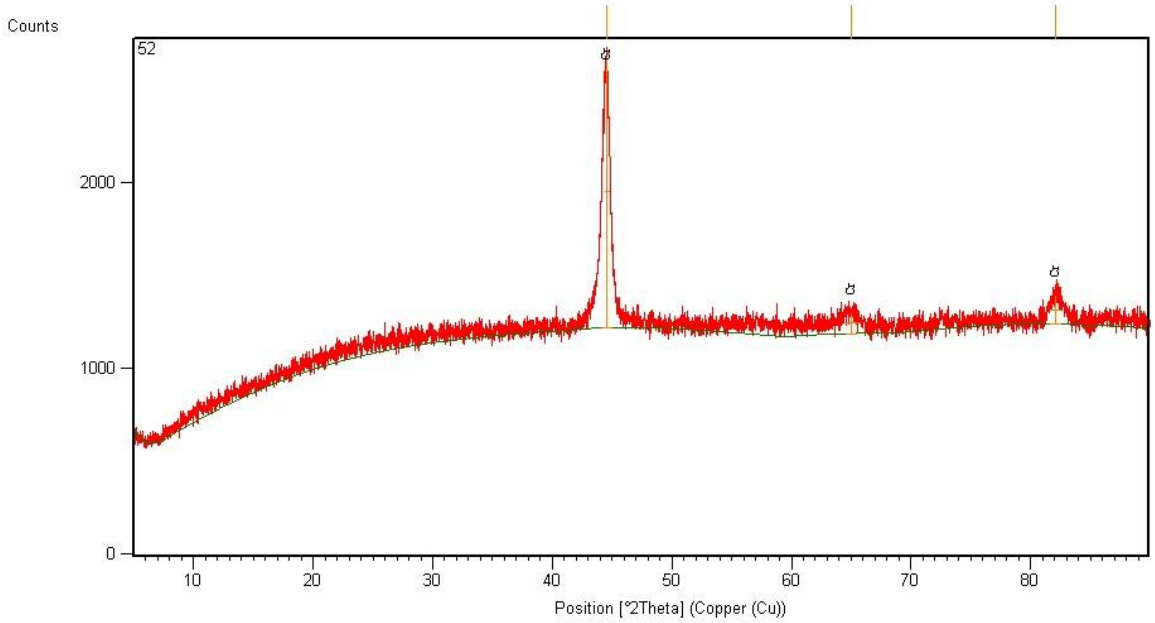

Figure 6.4: Peaks obtained for sample number 52

It was found that after hardening and then turning transformation has taken place the following phases were found as shown in table 6.5

Table 6.5: XRD results of sample number 52

Ref.Code	Score	Compound Name	Scale Factor	Chemical Formula	Weight fraction (%)
00-006-0694	66	Chromium	0.873	Cr	100.0

In X-ray diffraction (figure number 6.4), Three peaks have been obtained in the 2θ span ranging from 10 to 90. From these peaks the maximum value of relative intensity [%] is 90.00 at the position [^{0}2Th.] of 44.5331 gives one assignment i.e. Cr.

After turning of EN 9 at 60 HRC it was found that the other phases disappeared and only chromium was found shown in table 6.5.

Sample SAE 8620: Turned without hardening

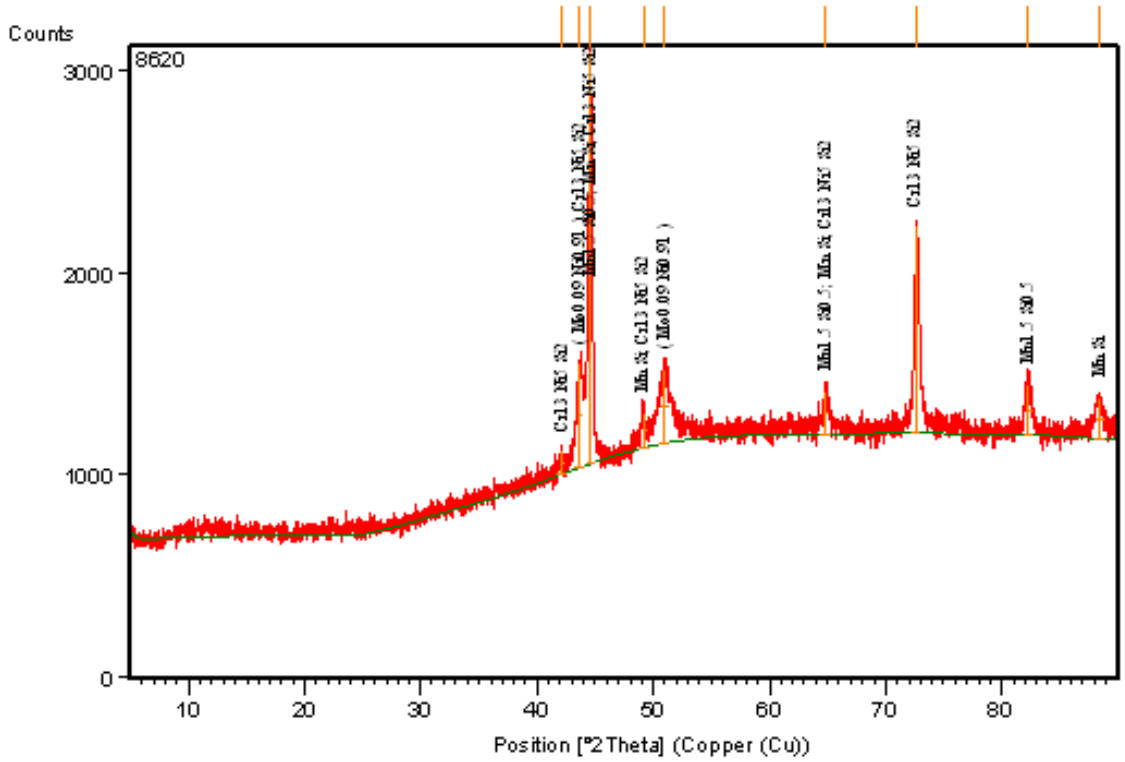

Figure 6.5: Peaks obtained for virgin sample SAE 8620

Table 6.6: XRD data for SAE 8620

Ref.Code	Score	Compound Name	Scale Factor	Chemical Formula	Weight fraction (%)
03-065-6979	73	Manganese Silicide	0.926	Mn_3 Si	4.0
01-071-7594	57	Molybdenum Nickel	0.260	$Mo_{0.09}$ $Ni_{0.91}$	1.0
00-054-0370	28	Manganese Silicon	0.829	Mn Si	6.0
00-054-0370	30	Chromium Nickel Silicon	0.747	Cr_{13} Ni_5 Si_2	89

Table number 6.6 shows the X-ray diffraction pattern of SAE 8620 (virgin sample), which show the presence of manganese silicide , molybdenum nickel, manganese silicon and Chromium Nickel Silicon .

In X-ray diffraction (figure number 6.5), Nine peaks have been obtained in the 2θ span ranging from 10 to 90. From these peaks the maximum value of relative intensity [%] is 100.00 at the position [^{0}2Th.] of 44.5432 gives two assignments i.e Mn_3 Si and Cr_{13} Ni_5 Si_2. The peaks in the pattern can be indexed to a mixture of different alloying elements and other remaining minor peaks attributed to impurity.

Sample number 49: After 60 HRC hard turning of SAE 8620

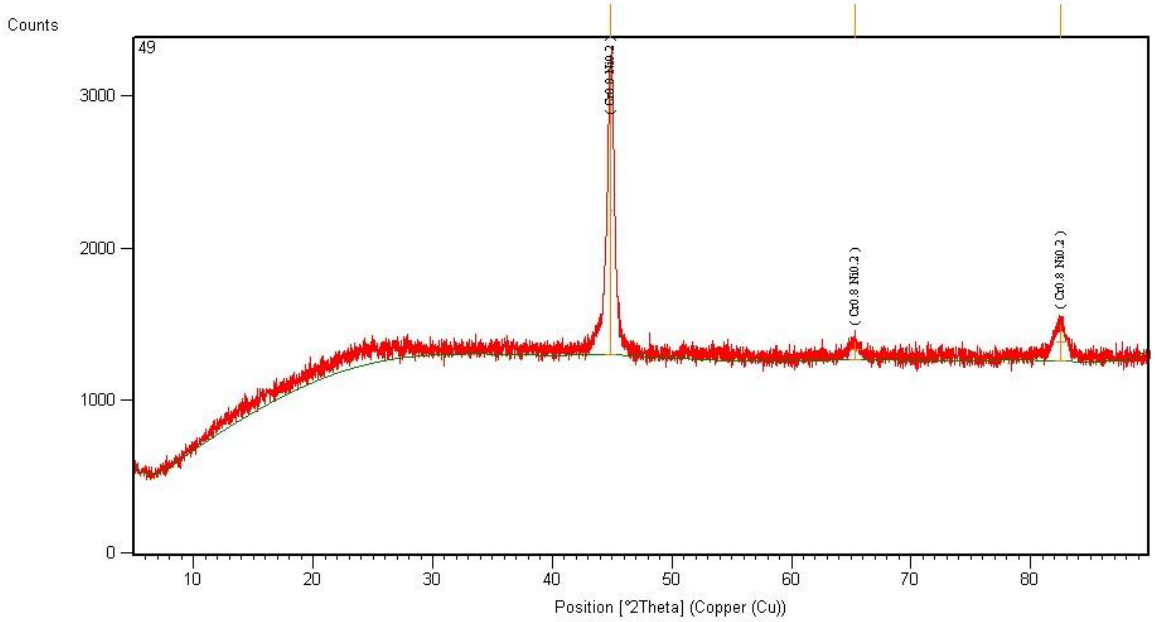

Figure 6.6: Peaks obtained for sample number 49

Table 6.7: XRD data for sample number 49

Ref.Code	Score	Compound Name	Scale Factor	Chemical Formula	Weight fraction (%)
01-071-7597	82	Chromium Nickel	0.873	$Cr_{0.8}$ $Ni_{0.2}$	100.0

In X-ray diffraction (figure number 6.6), Three peaks have been obtained in the 2θ span ranging from 10 to 90. From these peaks the maximum value of relative intensity [%] is 90.00 at the position [^{0}2Th.] of 44.8229 gives one assignment i.e. $Cr_{0.8}$ $Ni_{0.2}$.

After turning of SAE 8620 at 60 HRC it was found that the other phases disappeared and only chromium nickel was left as shown in table 6.7.

Table 6.8: Comparison of phases formed after hard turning and before hardening.

Material	Before hardening.	After hard turning
EN 31	Manganese Silicide , Silicon	Chromium
EN 9	Manganese Silicide, Chromium Nickel, Chromium Nickel Silicon	Chromium
SAE 8620	Manganese Silicide, Molybdenum Nickel, Manganese Silicon , Chromium Nickel Silicon	Chromium Nickel

Table 6.8 shows the final phase formed after and before hard part turning. It was found that in all the materials the final phase mainly comprised of Chromium. The initial phases of all samples were different. But the final phase of all material had the same constituent

6.4 CALCULATION OF MICRO STRAIN AND CRYSTALLITE SIZE

To calculate micro strain and crystallite size Devy Scherrer equation was used

Using the equation $$\frac{\beta\cos(\theta)}{\lambda} = \frac{1}{L} + \frac{\varepsilon \sin(\theta)}{\lambda}$$

β is full width at half maximum of the diffraction peaks. This can be expressed as a linear combination of the contributions from the strain (ε) and crystallite size (L)

λ is a constant 1.54 A (*Angstrom)*

The intercepts on the (β cos (θ)) axis equals to λ/L which gives the average crystallite size of the prepared sample. The strain rate is also calculated using the above equation which is equal to the slope of the plot. To calculate this ORIGIN 8 software was used. Table 6.9 shows the micro strain on the surface. [56]

Table 6.9: shows the micro strain and the Crystallite size of the samples

Sample	**Material**	**Micro Strain (ε)**	**Intercept = λ/L**	**Crystallite size = L(Angstorm)**
46 (60 HRC)	EN 31	-106.607	1.2456	1.236352
49 (60 HRC)	SAE 8620	-243.93	1.47939	1.04097
52 (60 HRC)	EN 9	-86.034	1.19542	1.28825
Virgin sample of EN 31	EN 31	-41.104	1.04105	1.479276
Virgin sample of EN 9	EN 9	-75.928	0.95644	1.610138
Virgin sample of SAE 8620	SAE 8620	-30.546	0.93639	1.644614

The – sign shows that compressive strain was present on the surface. The crystallite size decreased after hard turning.

6.5 COMPARISON BETWEEN HARD TURNED SURFACE AND GRINDING FINISH SURFACE

To study the surface of hard part turned material three samples were selected at different hardness and different materials. The fourth sample of SAE 8620 on which finish grinding was done using cylindrical grinder. It was observed that feed marks were generated on the surface of hard turned component. A uniform pattern was generated on the surface shown in figure 6.7 - 6.12. But on the grinded material an irregular pattern was generated as shown in the figure 6.13 and 6.14.

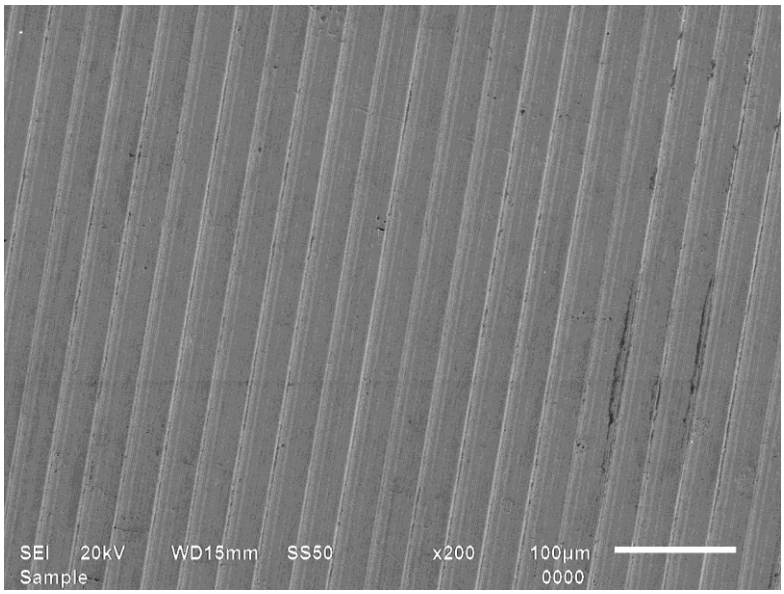

Figure 6.7: SEM image at 200 X for sample number 34

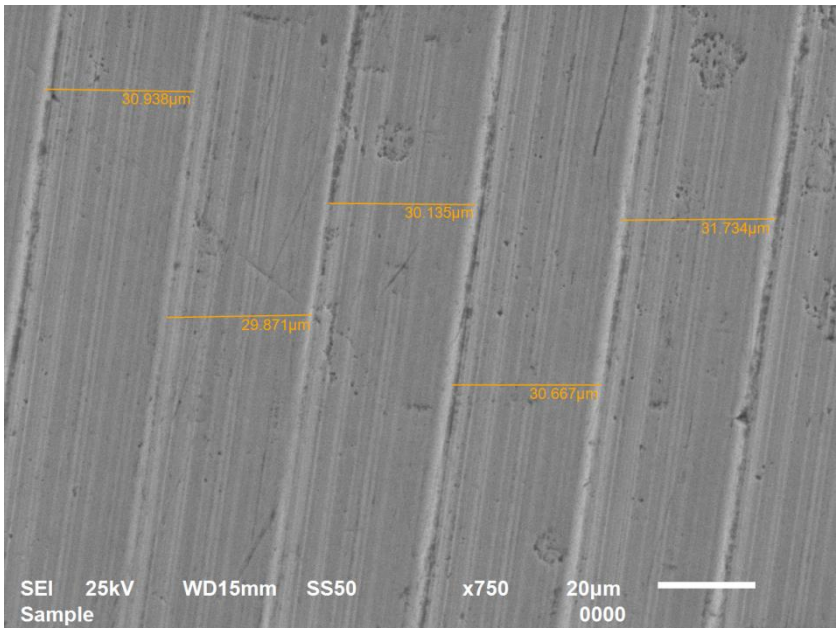

Figure 6.8: SEM image at 750 X for sample number 34

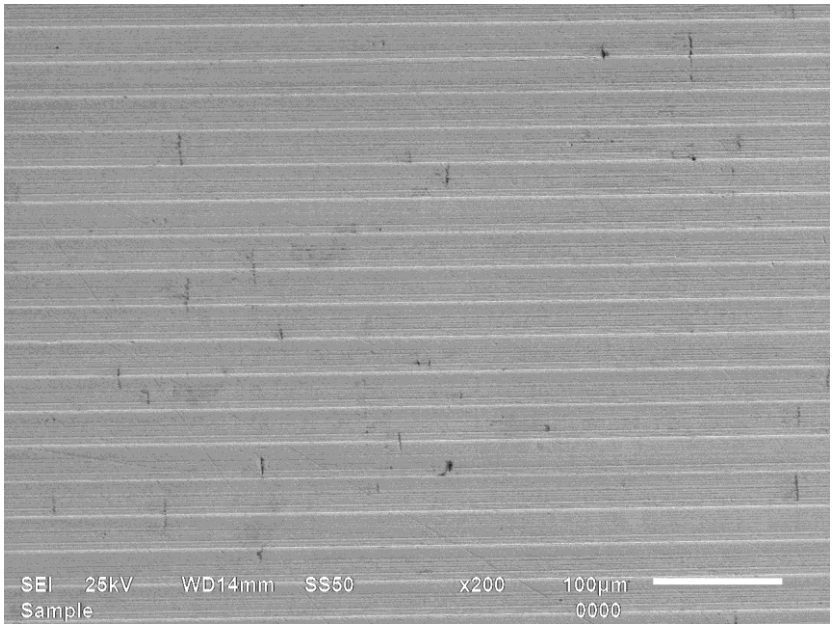

Figure 6.9: SEM image at 200 X for sample number 37

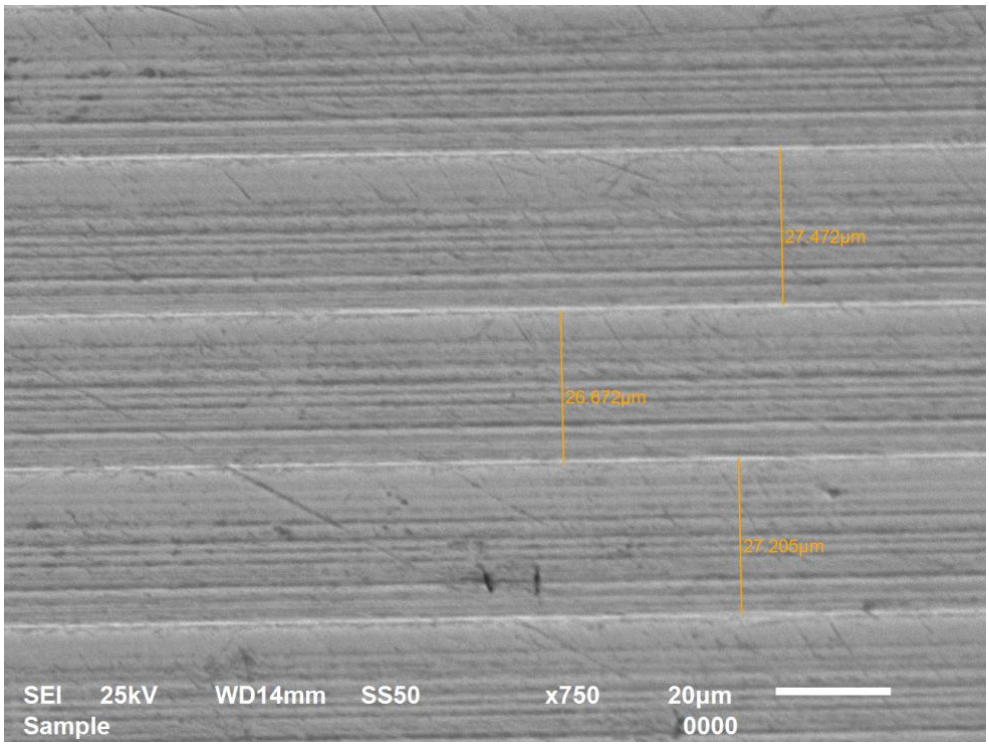

Figure 6.10: SEM image at 750 X for sample number 34

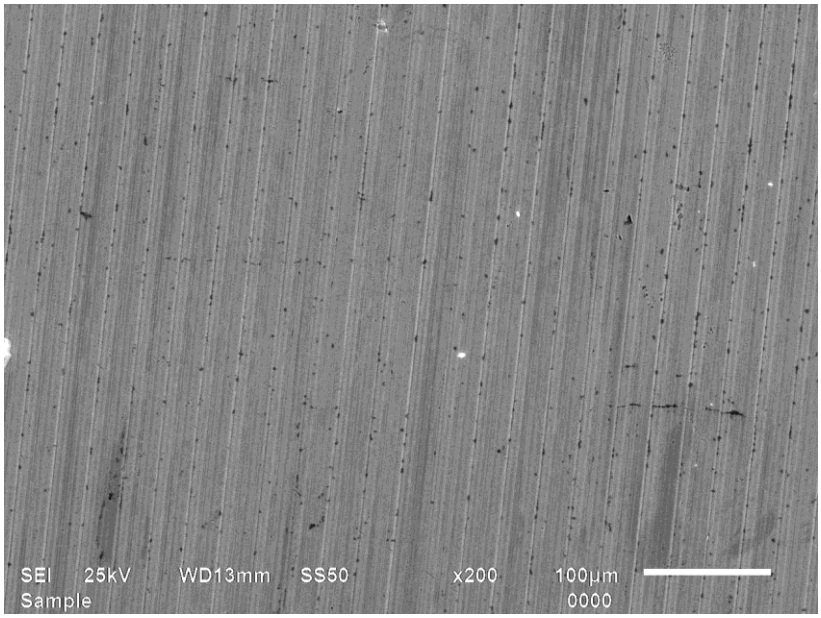

Figure 6.11: SEM image at 200 X for sample number 47

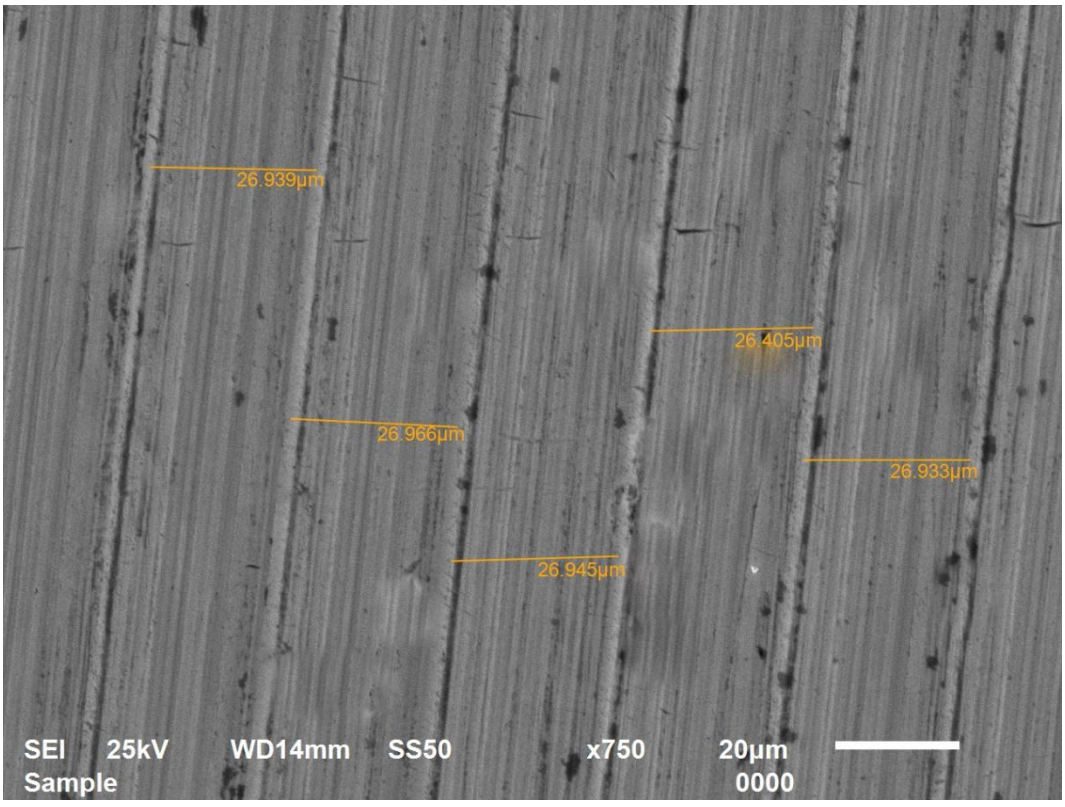

Figure 6.12: SEM image at 750 X for sample number 47

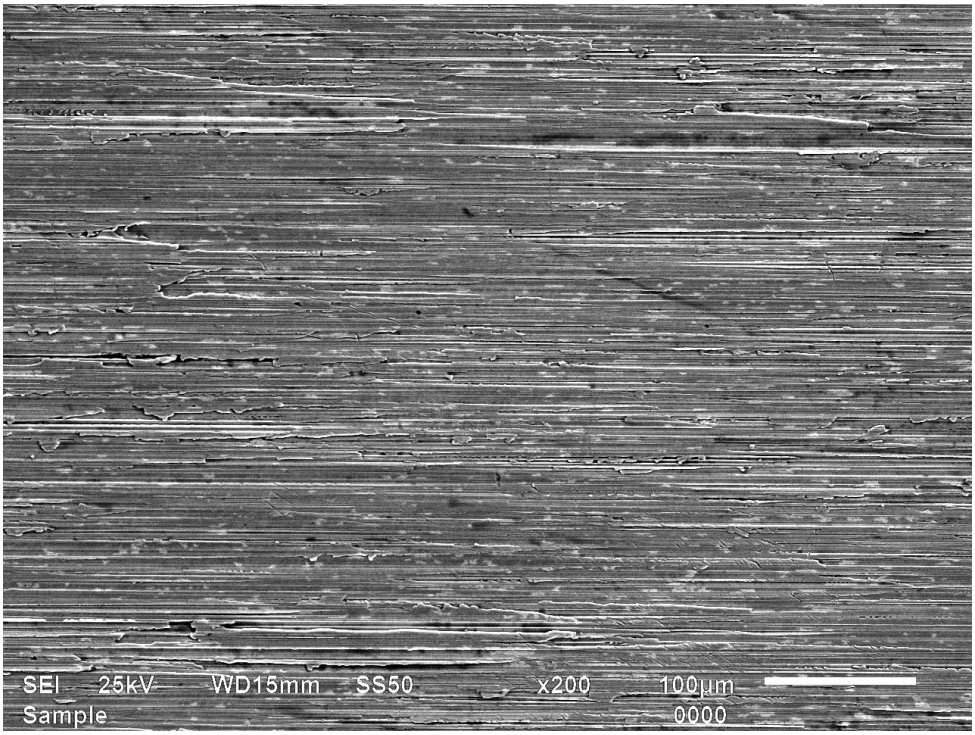

Figure 6.13: SEM image at 200 X for grinded sample

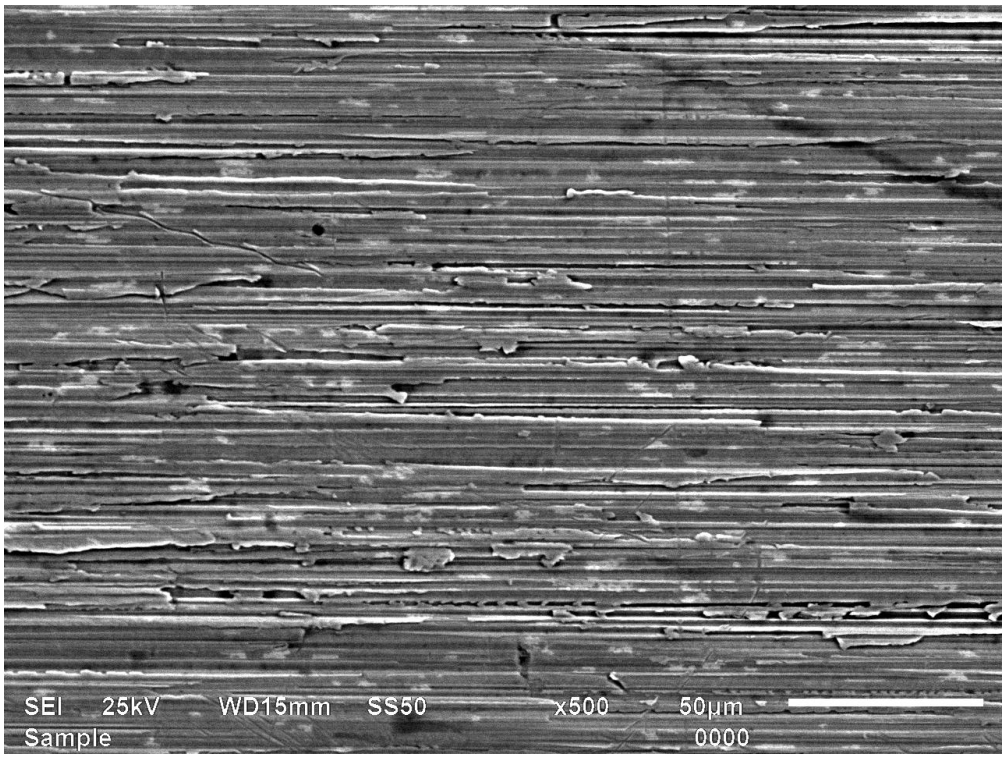

Figure 6.14: SEM image at 500 X for grinded sample.

6.6 WHITE LAYER FORMATION

White layer is the top layer formed on the surface of the hard turned component due to phase transformation. The white layer formed was between 7 to 10 microns. It is believed that white layer is formed because of rapid heating and quenching. Leica microscope was used to observe the white layer formation. Only selective samples shown in table 6.1 were selected for the study which had the best surface finish. Following steps were taken to prepare the specimen.

1. The shaft was cut using a parting wheel to make the specimen.
2. On the surface grinder machine the specimen ends were made parallel.
3. After this the ends were polished on a polishing machine.
4. Nitric acid etchant was applied on one end on which the white layer formation was to be studied.
5. After 2 minutes etchant was washed using spirit and the specimen becomes ready.
6. Place the specimen on the microscope and set a magnification of 400X.
7. Adjust the focus to clearly distinguish the white layer.
8. Use the microscope connected computer to capture the image. The name of software was AnviCam

Though the results were not so accurate but the thickness of white layer was measured using Metallurgical Image Analysing software (MIAS). The figures 6.15, 6.16 and 6.17 were analysed by using MIAS, The figures 6.18 and 6.19 were analysed using Leica microscopy.

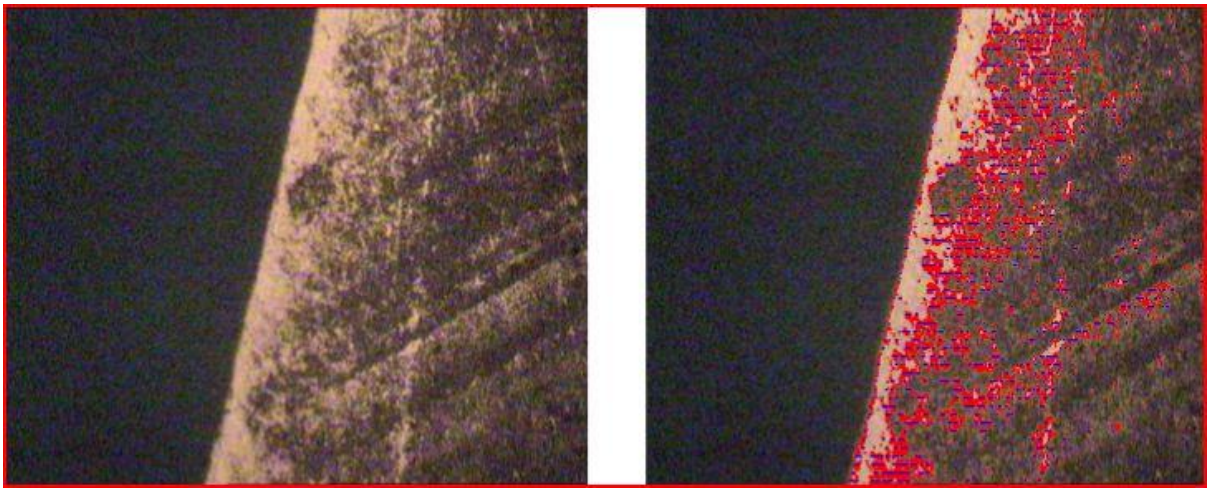

Figure 6.15: MIAS image for Sample number 34 at 400 X

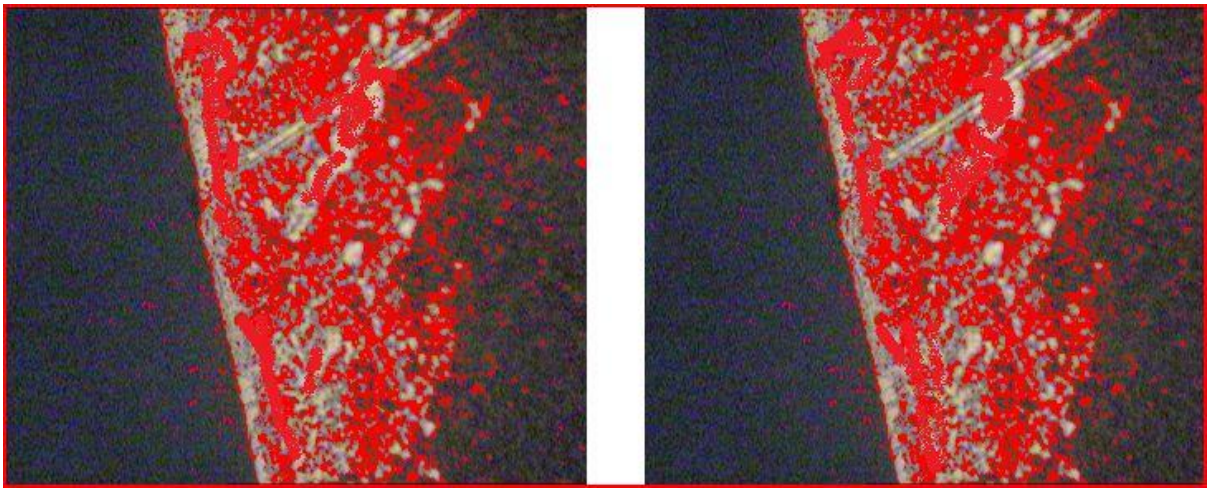

Figure 6.16: MIAS image for Sample number 37 at 400 X

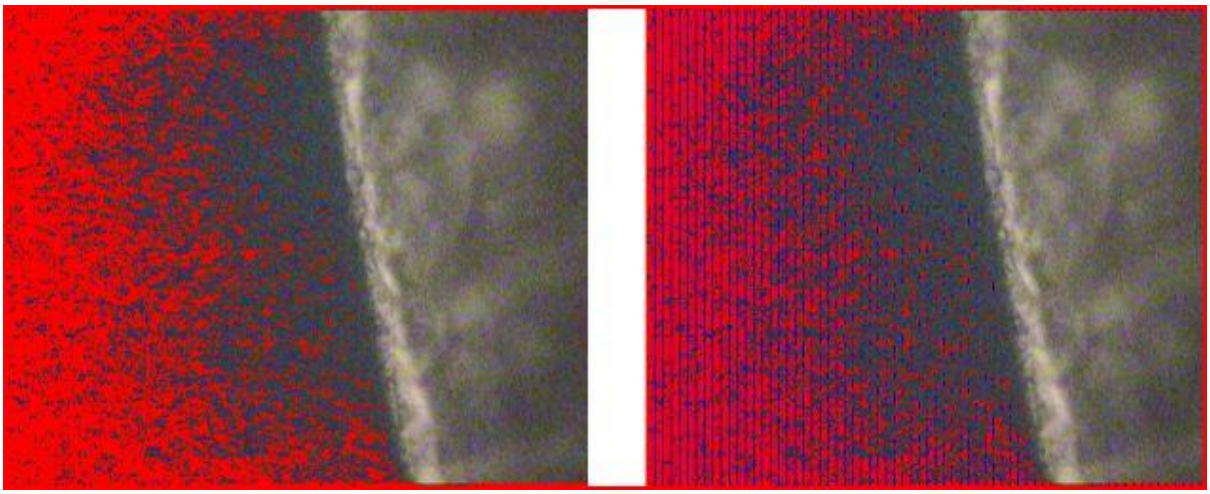

Figure 6.17: MIAS image for sample number 49 at 400 X

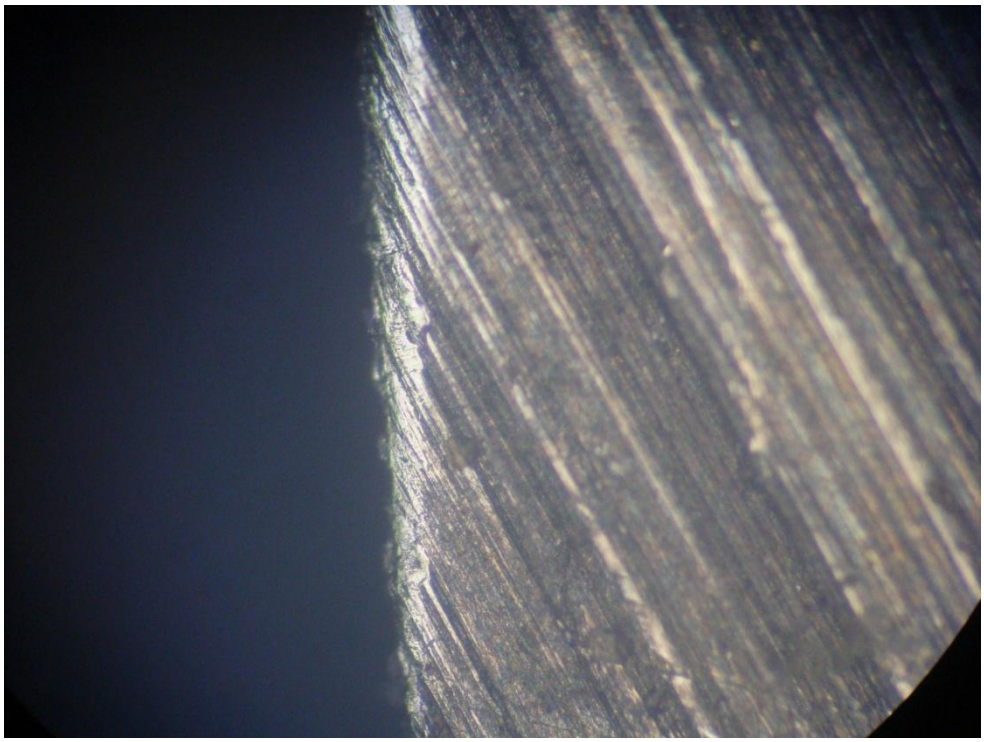

Figure 6.18: Leica microscope image of sample number 47 at 100 x

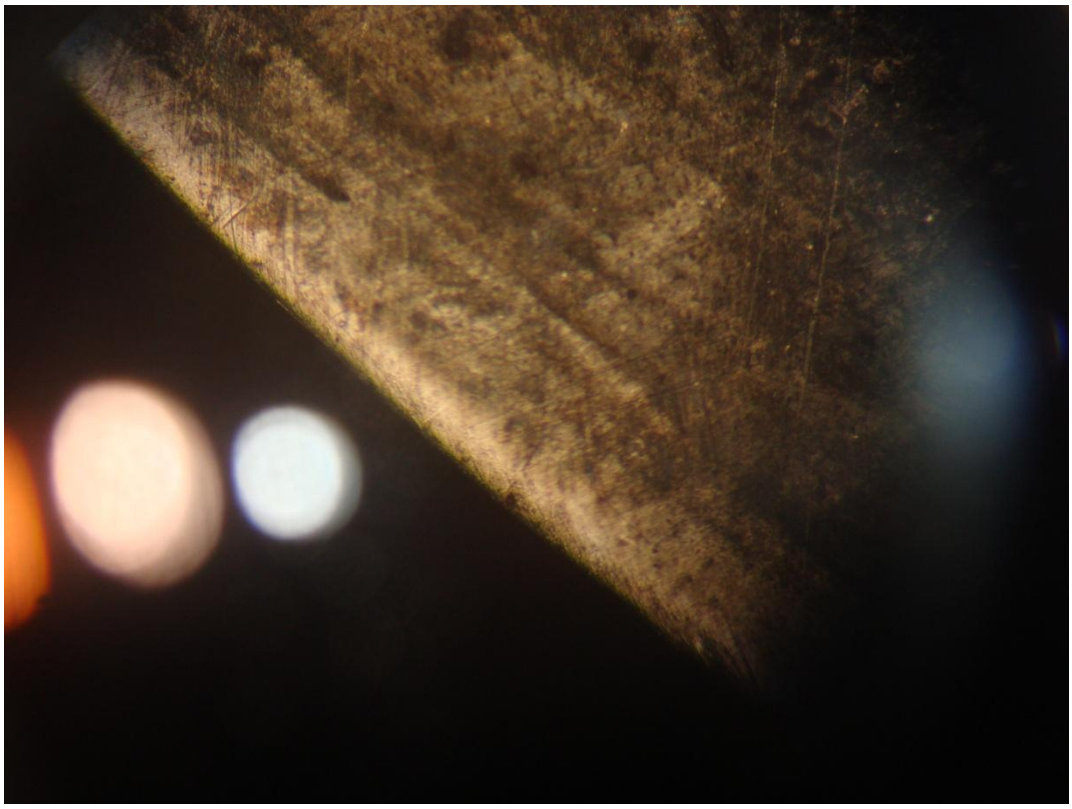

Figure 6.19: Leica microscope image of sample number 52 at 100 x

The three samples analysed using metallurgical image analysing software had following thickness shown in table 6.10.

Table 6.10: Thickness of white layer obtained from MIAS

Sample number	Thickness of the white layer in microns
34	9.56
37	9.12
46	7.4

It was found that the white layer was present in all the hard turned materials and MIAS gave an approximation of the layer thickness. Though it may not be very accurate way to measure the thickness but it gave an approximation of the layers formed.

CHAPTER 7

RESULTS AND CONCLUSIONS

7.1 RESULTS FOR FORCES AND SURFACE FINISH.

In the experiment Taguchi's L_{27} design was used to study the effect of hardness, material type, feed, cutting speed and the combined effect of nose radius and depth of cut on the machining forces, surface roughness, dimensional deviation, white layer formation and phase study. ANOVA was used to study the significance of various parameters. Grey relational analysis and Genetic Algorithm was used to design the optimum condition. From the experiment following results were obtained.

7.1.1 MACHINING FORCES

- The dynamometer readings showed that the main dominating force was radial force, tangential force was less than the radial force and feed force was the least. Upon this basis the machining force was mainly influenced by radial component of force.
- At feed rate of 0.03 mm/rev, forces were least. As the feed increased the forces also increased.
- The cutting velocity of 75 m /min it was observed that maximum force was applied there. As the working range of ceramic inserts was between 100 – 200 m /min. So ceramic inserts should be used in this specified range to get the best possible result.
- From 110 m /min to 150 m /min there was no considerable increase in the forces.
- Hardness played an important role in increase in the forces. The material type had no significant effect on machining forces.
- Nose radius of 0.8 mm had very small increase in the forces. Only depth of cut influenced the machining forces. As the depth of cut increased the machining forces increased.

7.1.2 SURFACE ROUGHNESS

- The best surface finish was obtained on the feed of 0.3 mm/rev.
- It was found that on some parameter settings the surface generated was very rough.
- Smaller depth of cut had much better surface finish.

- In comparison at same depth of cut the nose radius of 0.8 mm showed better results.
- To get better results cutting speed should fall in the working range of inserts.

7.1.3 DIMENSIONAL DEVIATION

- Digital vernier micrometer was used to measure the final diameter. It was found that the deviation was in the tolerance range of the h6 chart except on which very rough surface was generated.

7.1.4 GREY RELATIONAL ANALYSIS AND GENETIC ALGORITHM

- The grey relational analysis gave the best optimum combination of the input parameters. Equal weight age was given to all output response so GRA method was used.
- Genetic Algorithm generated a number of optimum solutions, to select the best one we have to decide on the basis of the importance of the output response required.
- Genetic Algorithm approach predicts the outputs which were not obtained by the grey relational analysis. Further results generated by Genetic Algorithm are very fast and précised.

7.1.5 TOOL WEAR

- All the insert edges were observed under the Leica Microscope and it was found that no wear take place on the flank face. But there was crater wear in some experiment.

7.2 METALLURGICAL ANALYSIS

7.2.1 XRD ANALYSIS

- It was found that before hardening samples and after hard turning samples there was a complete change in the phase.
- In different materials after hard turning on the most common element found was chromium.
- The compressive micro strain increased after hard turning in comparison to the virgin samples.
- The crystallite size decreased after hard turning.

7.2.2 WHITE LAYER FORMATION

- White layer does not get damaged due to the etching agent so it was possible to observe the white layer with help of Leica microscopy.
- MIAS software used gave results not so accurate but it was found that the white layer existed in microns.

7.2.3 SEM RESULTS

- SEM images showed that hard turned components showed a regular pattern, which was due to crest and trough formation.
- The centreless grinded component had a random pattern, which was due to the random orientation of abrasives in the grinding wheel.
- The distance between the lines (from on crest to another) was found to be approximately 30 microns which was same as the feed of 0.03 mm /rev.

7.3 CONCLUSIONS FROM FORCES AND SURFACE ROUGHNESS

It was found that to get the best results for hard part turning, to achieve best surface finish, and to minimise the machining forces it was necessary that the ceramic inserts used should be in there working range of 100 m /min to 200 m /min and the feed range of 0.03 to 1.5 mm/rev. 0.8 mm nose radius gave the best surface finish. Finishing cut along with less feed should be used to get the best surface finish. Roughing cuts can be given at high feed rate so that there is increase in production rate.

7.4 CONCLUSIONS FROM METALLURGICAL ANALYSIS.

XRD results showed that there was complete change in the phases. The main phase found was Chromium after hard turning of all materials. White layer does not get damaged by etching. The possible reason for the white layer formation was because of Heat affected zone (HAZ) or due to quenching. Distance between two crests was equal to the feed. Micro strain developed on the surface was compressive in nature and the main reason for this can be because of the formation of white layer.

7.5 SCOPE FOR FUTURE WORK

Further investigations are needed to develop the tool material inserts which should be comparatively cheap and last long. Apart from this, work should be done on development of cooling systems for the hard part turning process. So that white layer formation can be minimized. More study is to be done on metallurgical phase changes at different hardness for different materials after and before hard turning. Hard components having larger inner diameters gives roundness errors after hard turning, so work can be done to reduce the roundness errors of shafts by designing a special type chuck which imparts a uniform clamping force on the outer periphery.

REFERENCES

[1] http://www.engineershandbook.com/MfgMethods/ accessed on 23rd November, 2010

[2] Production technology by R.K Jain, Khanna publishers. ISBN 81-7409-099-1

[3] http://en.wikipedia.org/wiki/Turning accessed on 20th November, 2010

[4] Manufacturing automation: metal cutting mechanics, machine tool vibrations and CNC design By Yusuf Altintas Cambridge university press 2000

[5] American society for metals handbook, volume 3- 8th edition

[6] Textbook of production engineering by K. C. Jain, Chitale A. K , PHI learning , ISBN: 978-81-203-3526-4.

[7] http://www.mech.unimelb.edu.au/manuf-sci3/436413/tool_wear.htm accessed on 25th November, 2010

[8] http://www2.coromant.sandvik.com/coromant/pdf/Hard_part_turning/C-1040-069.pdf Sandvik coromant hard part turning journal accessed on 20th November, 2010

[9] Hemburg machine tools page http://www.hembrug.com/page.aspx?PageID=11 accessed on 20th November, 2010

[10] http://www.hardinge.com/usr/pdf/hardturn/ASME.pdf accessed on 20th November, 2010

[11]http://www.fandmmag.com/publication/article.jsp?pubId=1&id=504&pageNum=1 Fabricating and metalworking- march 2002 issue – magazine article- tips on hard turning by Mike Riley. Accessed on 20th November, 2010.

[12] American machinist http://www.americanmachinist.com/304/Issue/Article/False/67704/Issue accessed on 21st November, 2010

[13] Machinery's handbook 24th edition, industrial press inc, isbn 0-8311-2492-X

[14] http://www.ntkcuttingtools.co.uk/Ceramics.html accessed on 4th June, 2011

[15] Navas,V.G., García-Rosales,C., Sevillano, J.G., Ferreres, I. and Marañón, J. A.(2008) ' Hard part turning plus grinding-A combination to obtain good surface integrity in AISI 01 tool steel machined parts', *Machining Science and Technology*, vol 12: 1: pp. 15 - 32.

[16] http://carbideinserts.blogspot.com/2008/04/ceramic-inserts-vs-cbn-inserts.html acessed on 4th June, 2011.

[17] Gaitonde,V.N., Karnik,S.R., Figueira,L and Davim,J.P.; (2009) 'Analysis of Machinability During Hard Turning of Cold Work Tool Steel (Type: AISI D2)', *Materials and Manufacturing Processes*, vol 24: 12: pp. 1373 - 1382.

[18] Singh,D. and Rao,P.V.; *(2007)* 'A surface roughness prediction model for hard turning process' *International Journal of Advanced Manufacturing Technology vol* 32: pp. 1115 – 1124.

[19] Singh,D. and Rao, P.V.; (2007) 'Optimization of Tool Geometry and Cutting Parameters for Hard Turning', *Materials and Manufacturing Processes*, vol 22: 1: pp. 15 - 21.

[20] Chavoshi,S. Z, and Tajdari,M.; (2009) 'Surface roughness modelling in hard turning operation of AISI 4140 using CBN cutting tool' wear' *International Journal of Material Forming,* DOI 10.1007/s12289-009-0679-2.

[21] Zhang,J.Y. and Liang,S.Y.; (2007) 'Process Optimization of Finish Turning of Hardened Steels', *Materials and Manufacturing Processes*, vol 22: 1: pp. 107 - 113.

[22] Ozel,T., Hsu,T.K., Zeren,E.; (2005) 'Effects of cutting edge geometry, workpiece hardness, feed rate and cutting speed on surface roughness and forces in finish turning of hardened AISI H13 steel', *International Journal of Advanced Manufacturing Technology,* vol 25: pp. 262 – 269.

[23] Jang,D.Y. and Hsiao,Y.T.; (2000) 'Use of Ceramic Tools in Hard Turning of Hardened AISI M2 Steel', *Tribology Transactions*, vol 43: 4: pp. 641 - 646.

[24] Qian,L. and Hossan,M.R.; (2007) 'Effect on cutting force in turning hardened tool steels with cubic boron nitride inserts', *Journal of Materials Processing Technology*, vol 191: pp. 274 – 278.

[25] Sieben,B., Wagner,T. and Biermann,D.; (2010) ‘Empirical modeling of hard turning of AISI 6150 steel using design and analysis of computer experiments’, *Production Engineering Research Development*, vol 4: pp. 115 – 125.

[26] Cappellini,C., Attanasio,A., Rotella,G. and Umbrello,D.; (2010) ’Formation of dark and white layers in hard turning: influence of tool wear’, *International Journal of Material Forming,* vol. 3 Suppl 1: pp. 455 – 458.

[27] Aramcharoen,A. and Mativenga,P.T.; (2008) ‘White layer formation and hardening effects in hard turning of H13 tool steel with CrTiAlN and CrTiAlN/MoST-coated carbide tools’ -*Manufacturing & Laser Processing Group, International Journal of Advanced Manufacturing Technology,* vol. 36: pp. 650 – 657.

[28] Thamizhmanii,S. and Hasan,S.; (2009) ’Effect of tool wear and forces by turning process on hard AISI 440 C and SCM 440 materials’ ; *International Journal of Advanced Manufacturing Technology*, Vol. 2 Suppl 1: pp. 531 – 534.

[29] Sales,W.F., Costa,L.A., Santos,S.C., Diniz,A.E., Bonney,J., Ezugwu,E.O.; (2009) ‘Performance of coated, cemented carbide, mixed-ceramic and PCBN-H tools when turning W320 steel’- *International Journal of Advanced Manufacturing Technology,* vol 41: pp. 660 – 669.

[30] Ko,T.J. and Kim,H.S.; (2001) ‘Surface Integrity and Machinability in Intermittent Hard Turning’- *International Journal of Advanced Manufacturing Technology,* vol 18: pp. 168 – 175.

[31] Aslan,E., Camuscu,N. and Birgoren,B.; (2007) ’Optimization of cutting parameters when turning hardened AISI 4140 steel (63 HRC) with Al2O3 + TiCN mixed ceramic tool’ *Materials and Design, vol* 28: pp. 1618 – 1622.

[32] Zhang,J.Y., Liang,S.Y., Zhang,G. and Yen,D.; (2006) 'Modeling of Residual Stress Profile in Finish Hard Turning', *Materials and Manufacturing Processes*, vol 21: 1; pp. 39 - 45.

[33] Lalwani,D., Mehta,N.K. and Jain, P.K.; (2008) ‘Experimental investigations of cutting parameters influence on cutting forces and surface roughness in finish hard turning of MDN250 steel’- *Journal of materials processing technology, vol* 206 : pp. 167 - 179.

[34] Yallese,M.A., Chaoui,K., Zeghib,N., Boulanouar,L. and Rigal,J.F; (2009) 'Hard machining of hardened bearing steel using cubic boron nitride tool'- *journal of materials processing technology,* vol 209 : pp. 1092 - 1104.

[35] Zhou,J.M. and Hognas,S, (2010) ' Improving the waviness of bore in precision hard turning bu pressurized coolant'- *International Journal of Advanced Manufacturing Technology,* vol 49: pp. 469 - 474.

[36] Zhou,J. and Andersson,M.; (2007) 'Effects of Lubricant Condition and Tool Wear in Hard Turning of Novel-Abrasion-Resistance (N-AR) Cast Iron', *Materials and Manufacturing Processes,* vol 22: 7, pp. 865 - 870.

[37] Singh,D. and Rao, P.V.; (2008) 'Performance improvement of hard turning with solid lubricants', *International Journal of Advance Manufacturing Technology,* vol 38: pp. 529 – 535

[38] Pytlak,B.; (2010) 'Multicriteria optimization of hard turning operation of the hardened 18HGT steel', *International Journal Advance Manufacturing Technology,* vol 49: pp. 305 – 312.

[39] Kumar,CH R.V. and Ramamoorthy,B.; (2007) 'Performance of coated tools during hard turning under minimum fluid application' *Journal of Materials Processing Technology,* vol 185: pp. 210 – 216

[40] Chou,Y.K., Song,H.; (2004) 'Tool nose radius effects on finish hard turning', *Journal of Materials Processing Technology,* vol 148: pp. 259 – 268.

[41] Thamizhmanii,S., Kamarudin,K., Badrul,K., Saparudin,A., Hassan,S.; (2008) 'Study of Surface Roughness on Induction Hardened Steel using CBN Cutting Tool', *Proceedings of International Conference on Mechanical & Manufacturing Engineering,* Johor Bahru, Malaysia, ISBN: 97–98 –2963–59–2.

[42] Fnides,B., Yallese,M.A., Mabrouki,T., Rigal,J.F.; (2011) 'Application of response surface methodology for determining cutting force model in turning hardened AISI H11 hot work tool steel', *Sadhana,* Vol. 36:1; pp. 109 – 123.

[43] Yallese,M.A., Rigal,J.F., Chaouis,K., Boulanour,L., (2004) 'The effects of cutting conditions on mixed ceramic and cubic boron nitride tool wear and on surface roughness

during machining of X200Cr12 steel (60 HRC)', *Proceedings of the Institution of Mechanical Engineers, Part B: Journal of Engineering,* Vol. 219: 35.

[44] http://www.ee.iitb.ac.in/~apte/CV_PRA_TAGUCHI_INTRO.htm accessed on 4th June, 2011.

[45] http://www.chem.utoronto.ca/coursenotes/analsci/StatsTutorial/DegFree.html accessed on 4th June, 2011.

[46].http://www.efunda.com/materials/alloys/alloy_steels/show_alloy.cfm?id=aisi_8620&prop=all&page_title=aisi%208620, accessed on 2nd June, 2011

[47].http://www.efunda.com/materials/alloys/alloy_home/show_alloy_found.cfm?ID=AISI_1055, accessed on 2nd June, 2011

[48]http://www.efunda.com/materials/alloys/alloy_home/show_alloy_found.cfm?ID=AISI_52100, accessed on 2nd June , 2011.

[49] ACE CNC Jobber XL machine manual.

[50] Ingersoll catalogue-2011, www.ingersollcuttingtools.com/en/products/CAT-011_Technical.pdf, accessed on 7th June, 2011.

[51] www.coromant.**sandvik**.com/downloads , accessed on 7th June, 2011

[52] Kistler instrumente journal, 2005 http://www.kistler.com/mediaaccess/300-400e-07.09.pdf accesed on 23rd November, 2010

[53] Phillip J. Ross, Taguchi Techniques for Quality Engineering, *Mc Graw-Hill Book Company, Second Edition*, 1988.

[54] Tzeng,C.J., Lin,Y.H.,Yang,Y.K., Jeng,M.C., (2004) 'Optimization of turning operations with multiple performance characteristics using the Taguchi method and Grey relational analysis' *Journal of Materials Processing Technology*, Vol 209, pp 2753 – 2759

[55]http://serc.carleton.edu/research_education/geochemsheets/techniques/XRD.html,

acessed on 29th june 2011.

[56] prism.mit.edu/xray/CrystalSizeAnalysis.ppt accessed on 29th June, 2011.

[57]http://www.genetic-programming.com/gppreparatory.html

[58]http://en.wikipedia.org/wiki/Genetic_programming

[59]http://www.obitko.com/tutorials/genetic-algorithms/ga-basic-description.php

[60]Deb, Kalyanmoy. Multiobjective Optimization using Evolutionary algorithms. John wiley and sons 2001